LMSC-D973437

DEMONSTRATION OF TRANSPARENT SOLAR ARRAY MODULE DESIGN

JPL CONTRACT NO. 956608

GEORGE J. PACK

SEPTEMBER 1984

FINAL REPORT

This work was performed for the Jet Propulsion Laboratory, California Institute of Technology sponsored by the National Aeronautics and Space Administration under Contract NAS7-918.

LOCKHEED MISSILES & SPACE COMPANY, INC.
SPACE SYSTEMS DIVISION
SUNNYVALE, CALIFORNIA 94088-3504

ABSTRACT

This report discusses the design, development, abrication and testing of IR transparent solar array modules. Three modules, consisting of a baseline design using back surface reflector cells, and two modules using gridded back contact, IR transparent cells, were subjected to vacuum thermal balance testing to verify analytical predictions of lower operating temperature and increased efficiency. As a result of this test program, LMSC has verified that a significant degree of IR transparency can be designed into a flexible solar array. Test data correlates with both steady state and transient thermal analysis.

TABLE OF CONTENTS

ILLUSTRATIONS

Section 1
INTRODUCTION

Two of the major problems being addressed in solar array R&D are determining methods of maximizing specific power (w/kg) and power density (w/m^2). A key factor affecting the array performance and thus these two figures of merit is the operating temperature. It is a well known fact that the operating voltage and power are relatively strong functions of temperature. Maximizing power therefore implies minimizing the operating temperature.

As a result of research conducted under NASA technology contracts and internal ID funding, LMSC has developed a unique approach to minimizing the operating temperature. Previous efforts at improving the thermal characteristics have concentrated on increasing the reflectance or by absorbing and emitting at a longer wavelength. The solution developed at LMSC is to take advantage of the inherently low absorption coefficients of both silicon and gallium arsenide in the IR and, by proper choice of the other materials within the optical path, design an array which is highly transparent within the IR spectral region from $1.1 \leq \lambda \leq 4.0\,\mu$. Approximately 25% of the solar energy is contained within this interval which is outside of the solar cell conversion band. By careful choice of the materials used, a reduction in solar absorptance (α) to $\alpha = 0.60$ is achievable. Analysis of the array thermal and electrical performance shows a predicted operating temperature of 12°C and orbital efficiency of 14.5% for a 2 Ω-cm (13.5% efficient at T = 28°C) cell.

The objective of this project was to prove via thermal balance testing the effectiveness of an IR transparent array in reducing the operating temperature. Three test articles incorporating various degrees of transparency were fabricated and tested in vacuum to determine their operating temperature.

The following sections will discuss the design of the three test articles, their fabrication, test facilities, conduct of the test, results and data analysis.

Section 2
TEST ARTICLE DESCRIPTION

Three modules using four 5.9 x 5.9 cm^2 WAC (wraparound contact) solar cells were designed and fabricated for this test. Figure 1 shows the general mechanical configuration. Features common to all three modules include a black aluminum sunshade to minimize solar reflection in the chamber, a kapton printed circuit substrate and four 5.9 x 5.9 cm^2 WAC solar cells.

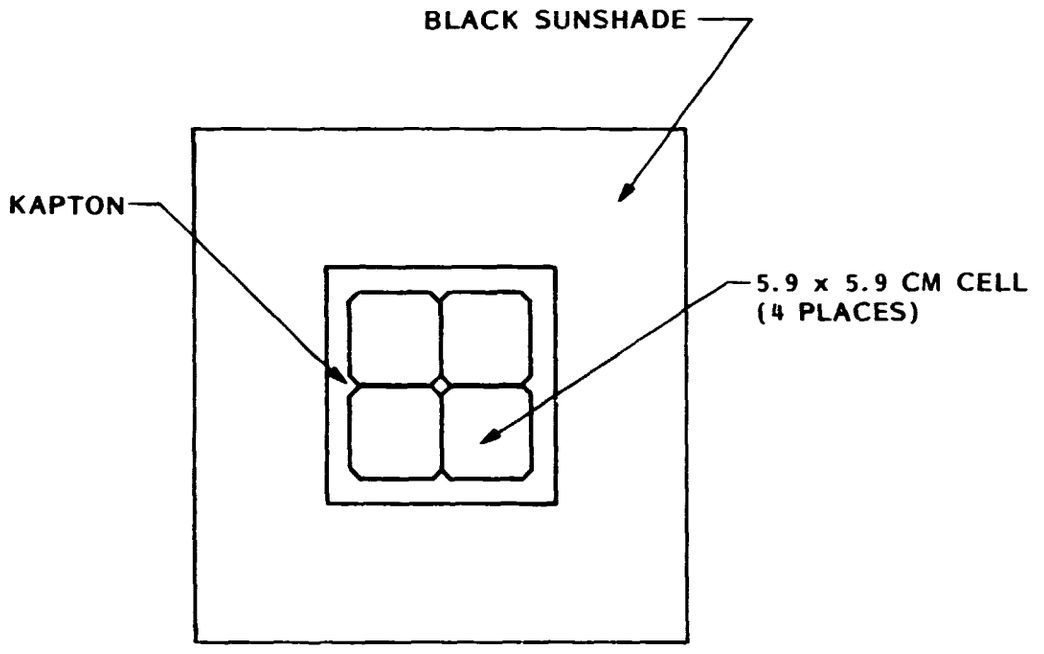

Figure 1 General Mechanical Configuration

The first module, designated module A, utilized several materials and design techniques intended to enhance transparency. A developmental gridded back contact cell with an SiO_2 antireflective coating on the back surface was chosen. The contact on this cell was designed to have a minimum amount of metal on the back surface

which would intrude into the optical path. The AR coating is a non-optimized, single layer filter with a central wavelength at $\lambda = 1.7\mu$. Copper circuitry, shown in Figure 2 was designed to overlay the cell gridlines or intercell spaces to minimize additional blockage. Wherever possible, any excess kapton which intruded into the optical path was cut out. The complete module is shown in Figure 3 (a) and (b).

Module B was designed along the same lines as the first module with two exceptions: the kapton substrate was not cut away and the cells were held down with an acrylic transfer tape. This design simulates a retrofit of the IR transparent cells to a flexible array constructed along traditional lines. Figure 4 (a) and (b) show the completed module.

The final module simulates the current optimum thermal design for a conventional flexible array. Cells chosen were 2 Ω-cm Back Surface Reflector (BSR) cells with a solar absorptance of $\alpha = .70$. These cells have no measureable transmittance and represent the current state of the art for reflector cells. The kapton printed circuitry was identical to that used in the other modules to maintain similar copper conduction and radiation areas. Bonding of the cell to the substrate was accomplished by using the same acrylic transfer tape used on module B. The cell bonding is required to raise the effective back surface emissivity (ϵ) from approximately $\epsilon = 0.25$ to $\epsilon = 0.80$. This final module C is shown in Figure 5 (a) and (b).

An important part of the design process was determining material properties and choosing those which were applicable. Appendix A lists the materials evaluated and their measured spectra. It was fortuitous that most of the materials currently being used for flexible arrays are at least marginally acceptable and in most cases quite good. As such, the modules utilized these qualified materials to provide a measure of "baseline" performance.

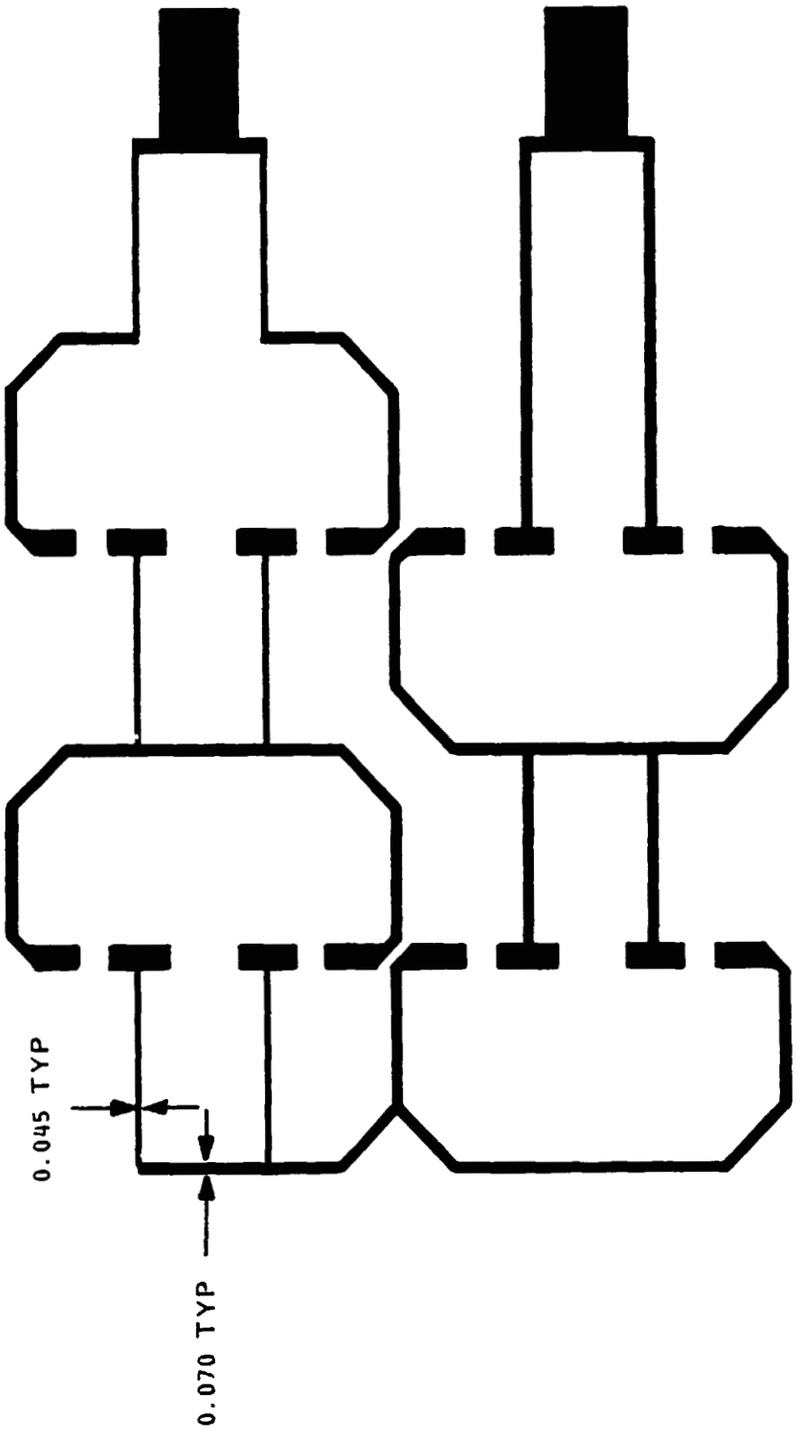

Figure 2 Transparent Module Interconnect

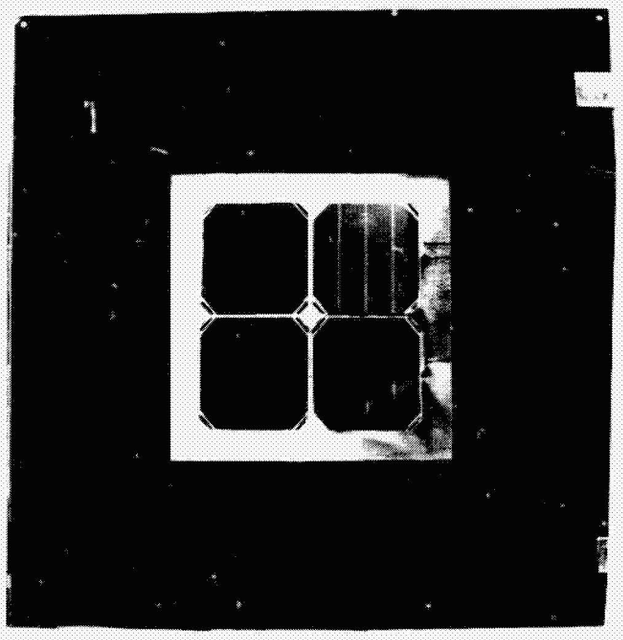

(a) Front

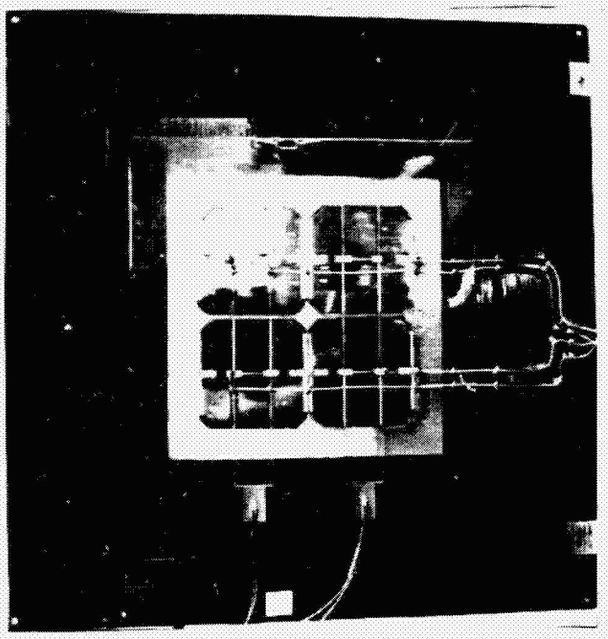

(b) Back

Figure 3 Module A

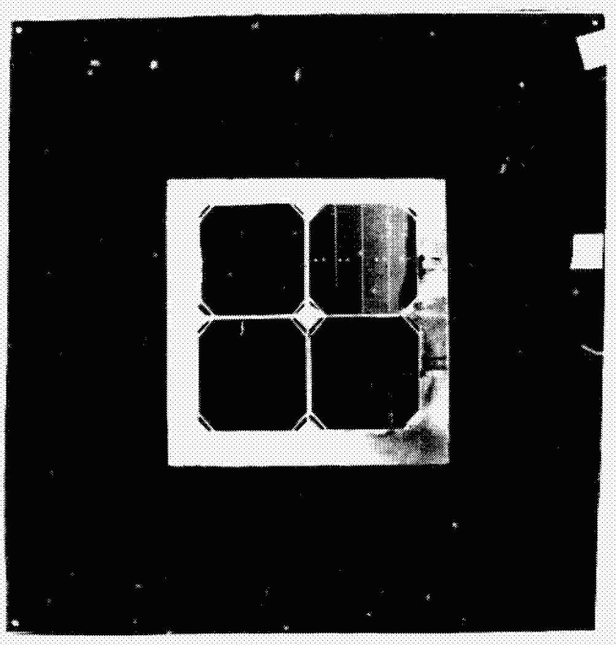

(a) Front

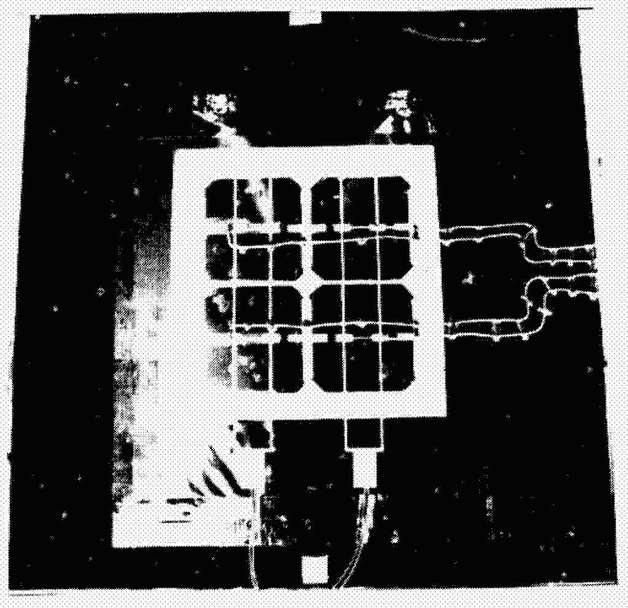

(b) Back

Figure 4 Module B

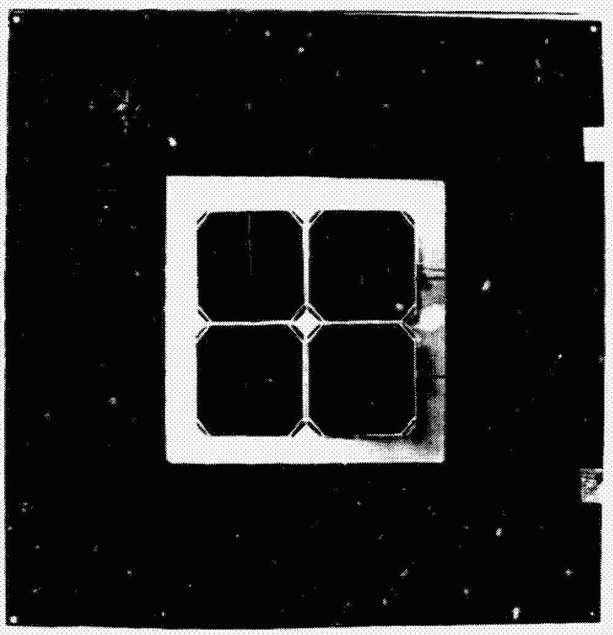

(a) Front

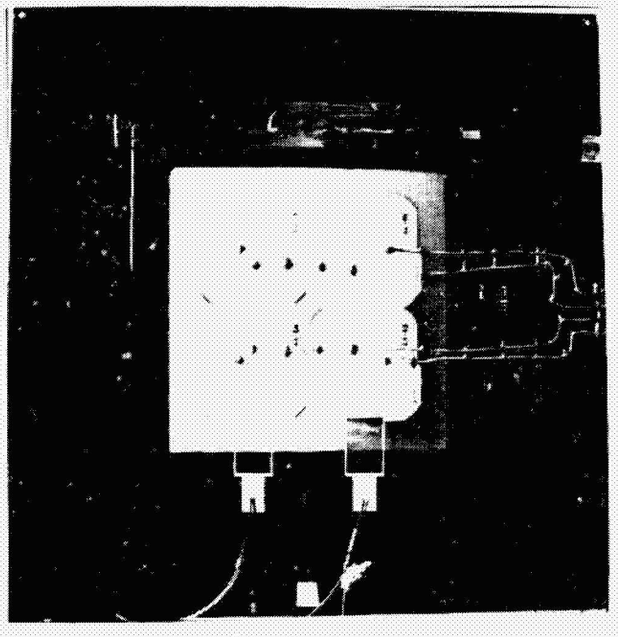

(b) Back

Figure 5 Module C

Materials chosen were:

- 0211 microsheet covers
- DC93-500 silicone adhesive
- Silicon cells
- Y9460 acrylic adhesive (modules B and C)
- Kapton/polyester/copper printed circuit substrate

It was originally intended to include a test sample incorporating gallium arsenide wafers assembled into a module configuration. An order was placed for 12 test waver assemblies which were to consist of a fused silica cover with AR-UV coatings, DC93-500 adhesive and a gallium arsenide blank polished on both sides with an AR coating applied to both surfaces. Reflectance and transmittance measurements were made on two of the wavers as received as shown in Figure 6. These measurements clearly showed a discrepancy between what was ordered and what was received. By using published values of the absorption coefficient for GaAs, the internal transmittance can be calculated to be $89\% \leq \tau \leq 98\%$ at $\lambda = 1.8\mu$ depending on doping density. Published data on a highly doped GaAs wafer gave the external transmittance at $\lambda = 1.8\mu$ as $\tau = 0.58\%$. Since the samples measured were AR coated and covered, the transmittance at $\lambda = 1.8\mu$ should range between $0.58\% \leq \tau \leq 0.98\%$. The measured value of $\tau = 18\%$ is significantly lower. Since the lead time for ordering and receiving additional wafers would extend the contract several months, it was decided to delete the GaAs module from this test program. JPL concurred with this decision.

Instrumentation for determining irradiance and temperature during the test consisted of two radiometers and four Cu-Co thermocouples per sample. Radiometer construction is shown schematically in Figure 7. Basic features incorporated into the design include a biasing heater for calibration, aluminum face sheets to provide an isothermal surface, two Cu-Co thermocouples for temperature measurement and a black thermal control paint to provide high α/ϵ (0.90/0.91).

Thermocouple locations for the test modules are shown in Figure 8.

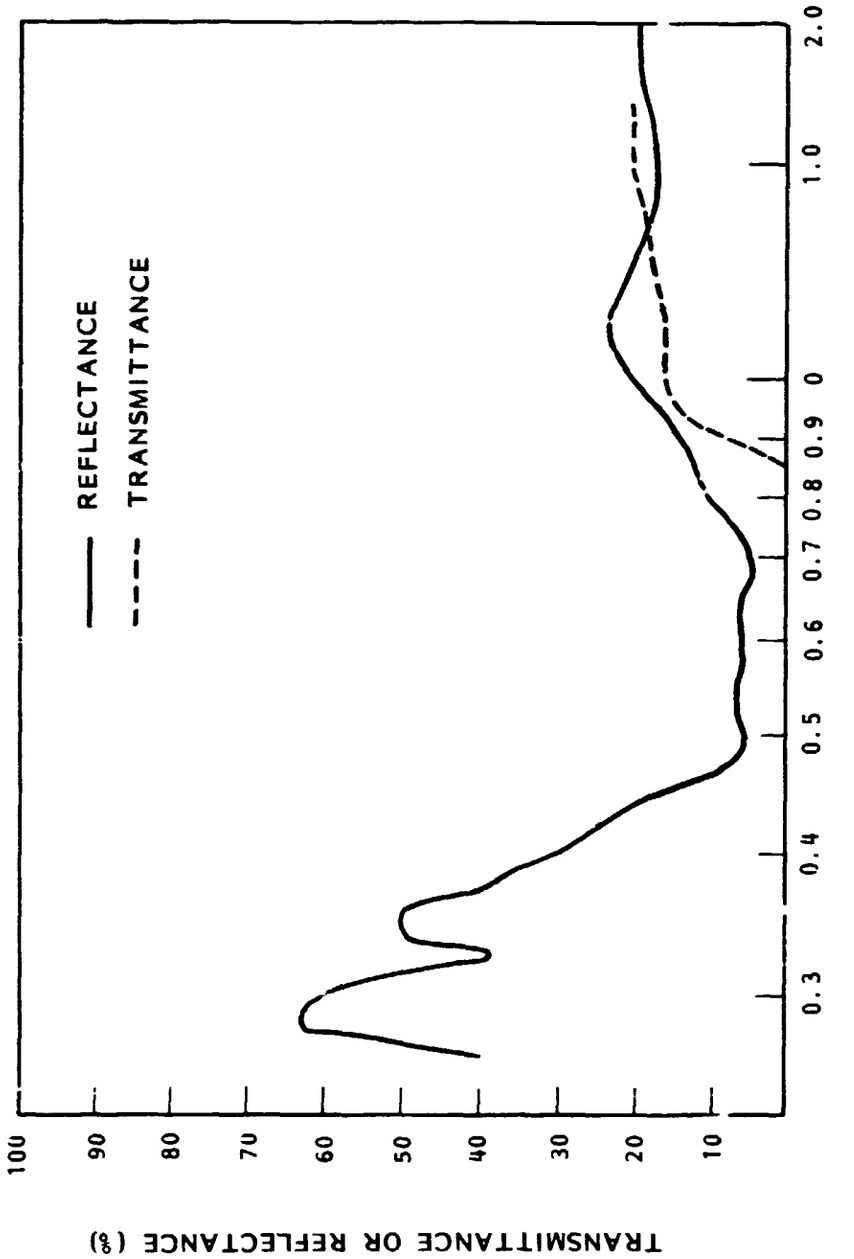

Figure 6 Transmittance and Reflectance of GaAs

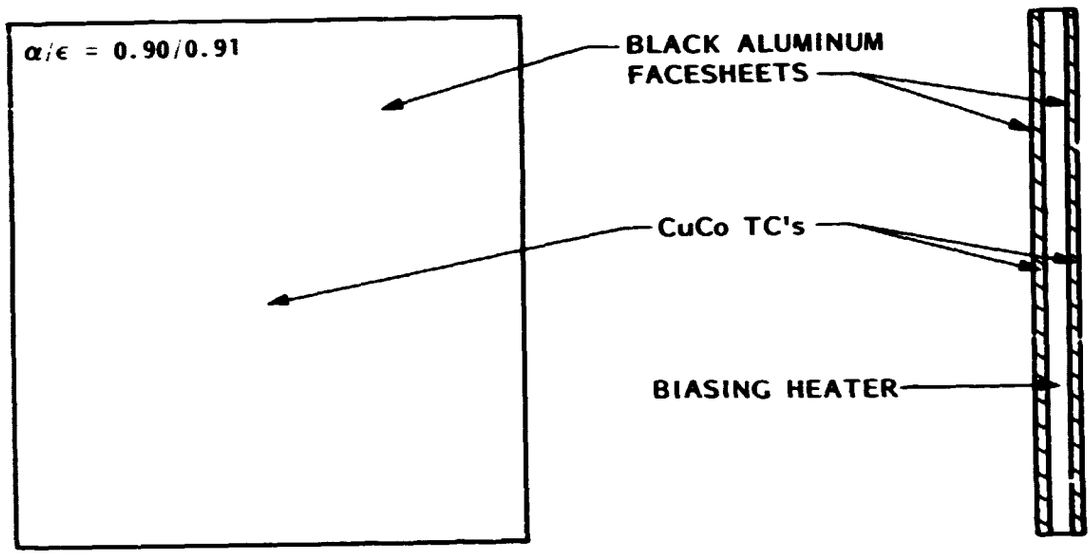

Figure 7 Radiometer Construction

TEST MODULE	THERMOCOUPLE NO.			
A	1	2	3	4
B	5	6	7	8
C	9	10	11	12

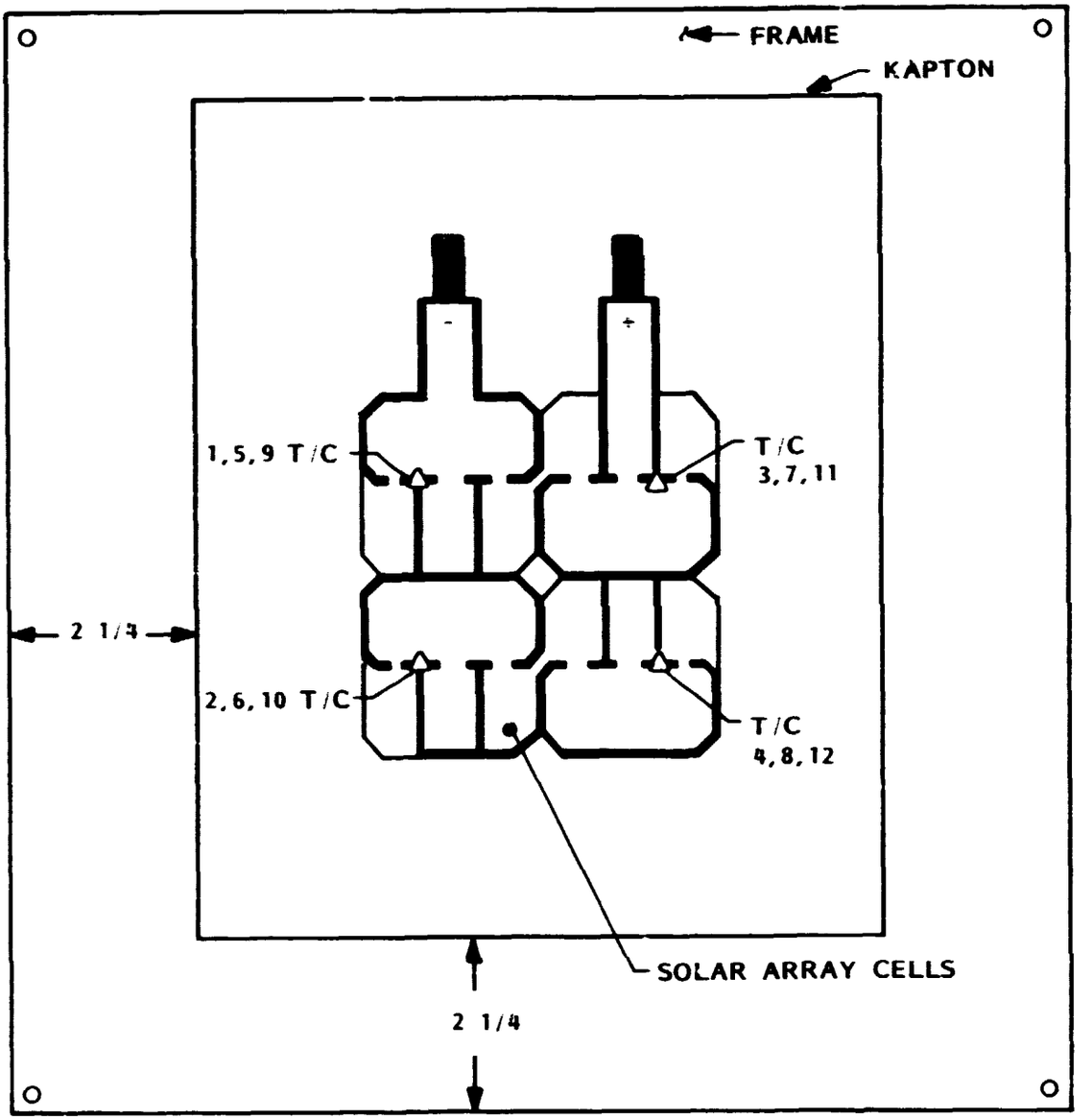

THERMOCOUPLES ON BACK OF KAPTON

Figure 8 Thermocouple Instrumentation - Back View

Section 3
TEST FACILITIES DESCRIPTION

All testing was done in an Ultek Space Simulation Vacuum Chamber, shown schematically in Figure 9, at LMSC. This chamber has a 57.0 in. diameter by 71.0 in. long working section surrounded by a liquid nitrogen shroud. All interior surfaces are painted with a black thermal control paint having a high α/ϵ (0.90/0.91). A mechanical roughing system with LN_2 cold trap is used for preliminary pumping with an ion pump used to achieve high vacuum. An 8.0 in. diameter ultra-violet grade window is provided in one side of the chamber wall. System pressure is continually monitored by two vacuum gauges. Liquid nitrogen shroud temperatures are monitored with seven Cu-Co thermocouples.

Insolation was simulated by a Spectrolab X-25 solar simulator. When set up properly, this simulator provides a close spectral match to the sun. AM0 solar intensity is achieved at a sample to simulator distance of 92.0 ± 4.0 in.

After testing it was discovered that the simulator's Zenon bulb had been incorrectly adjusted after installation. This results in a spectral shift towards the red. All material properties were reintegrated against this shifted spectrum for use during analysis.

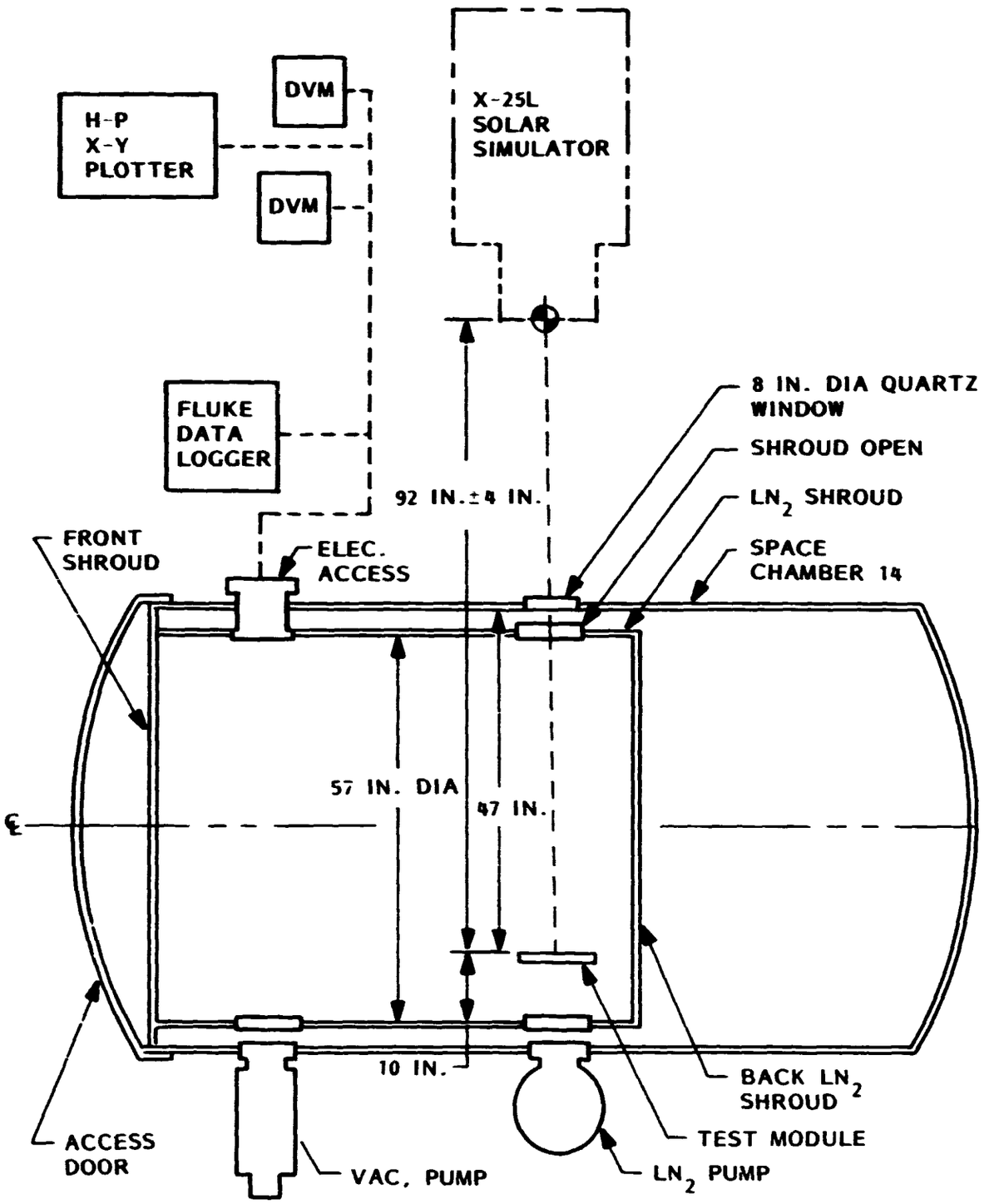

Figure 9 Schematic - Test Setup Space Chamber

Section 4
TEST CONDUCT

Testing was initiated on 21 February with the calibration of the chamber. For the chamber calibration a 4 x 4 in^2 black plate radiometer was mounted in a sun shade frame and installed in the chamber in the same location as the samples. The chamber was then sealed, a vacuum pulled and LN_2 introduced into the shrouds. Using the internal heater, a plot of temperature versus radiated power was determined. Figure 10 shows the results of this testing as well as pretest predictions. A similar test sequence was then initiated using the X-25 simulator as the heat source with the results shown in Figure 11. Combining these two sets of data yields the simulator adjustment versus power curve shown in Figure 12.

Each solar array segment was tested at three intensity settings corresponding to incident power densities of 0.1372, 0.1293, and 0.1012 W/cm^2 as determined from the calibration chart. Expressed as a fraction of the nominal solar constant these were 1.01, 0.96, and 0.75. At each setting the samples were allowed to approach equilibrium. A rough electrical characterization of each sample was also made at a setting of 0.1372 W/cm^2.

In order to obtain a quantitative measure of the transmitted energy, a black plate radiometer was mounted behind the array segment. The radiometer used was 3 x 3 in^2 and was positioned 4 in. behind the sample.

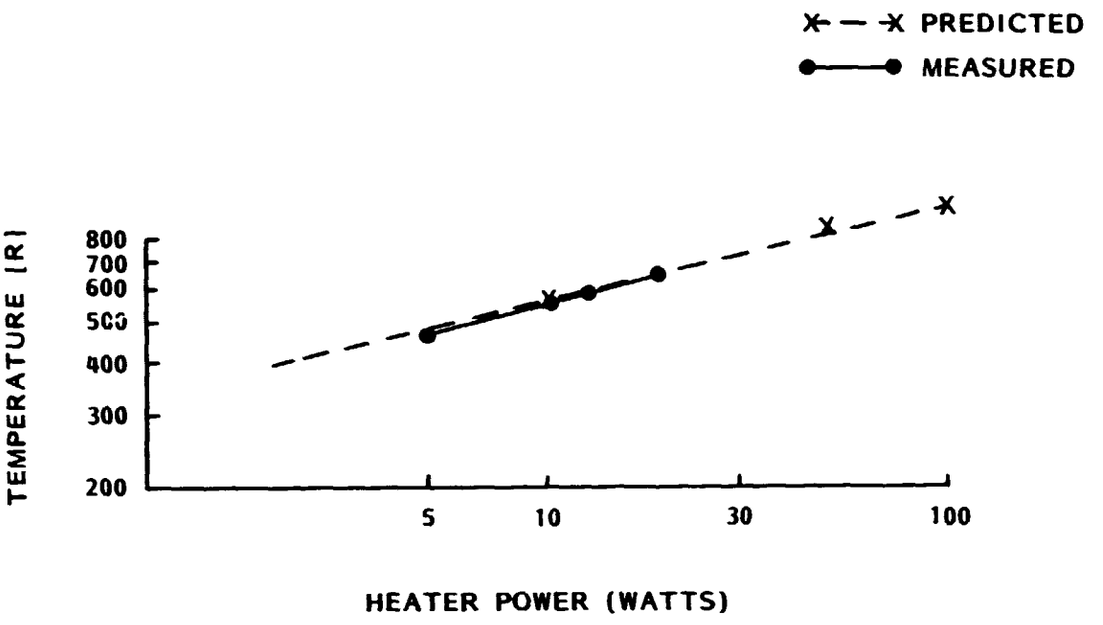

Figure 10 Radiometer Temperature vs Applied Heater Power

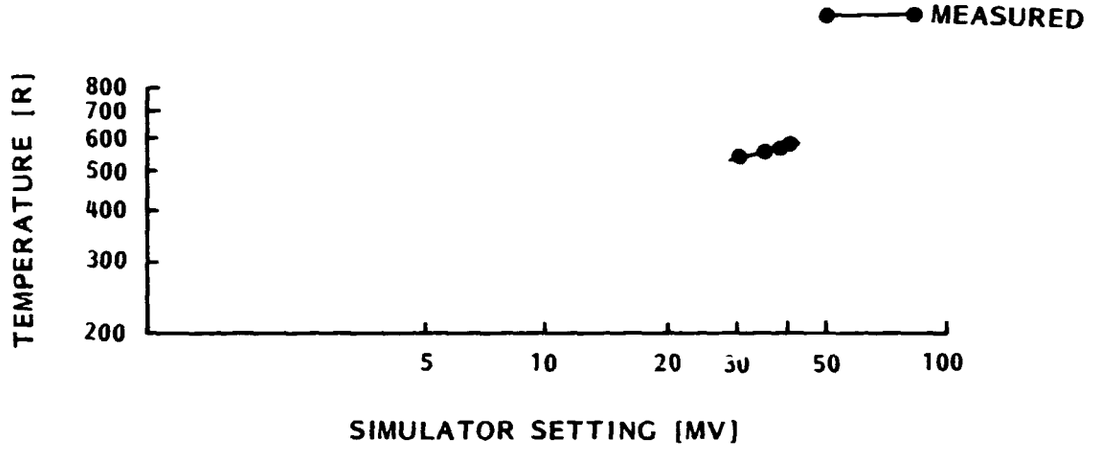

Figure 11 Radiometer Temperature vs Simulator Setting

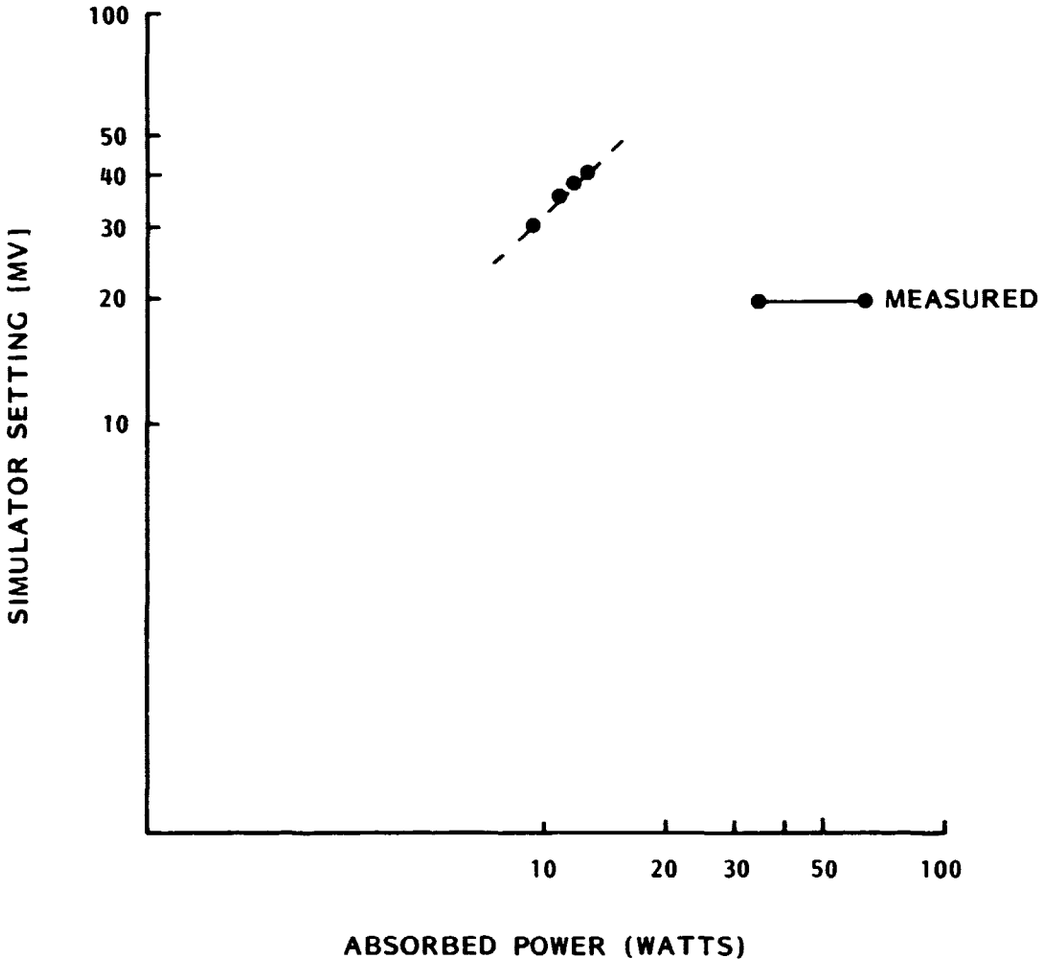

Figure 12 Simulator Setting vs Absorbed Power

Section 5
RESULTS

Results of the thermal balance testing and data analysis are shown in Figures 13 through 21. Due to the size and separation distance of the radiometer in relation to the sample, the resulting system was closely coupled thermally. Consequently, the key data to evaluate is the temp . ure of the radiometer. As an example, the radiometer on sample A ran at . : 1.01 solar constants while the radiometer on sample C was at -50°F. This 50°F change in radiometer equilibrium temperature represents the effects of the transmitted energy through sample A.

Two analytical thermal models, steady state and transient, were developed to interpret the test results. Figure 22 shows the six node thermal network which was used as the model in the analysis. All of the major heat transfer and energy storage terms are shown schematically. Generally good correlation between the test results and the analytical predictions was achieved for all samples and test conditions. Two perturbations shown in the figures are the result of varying the simulator setting during the test. In Figure 15, the setting was slightly low and was therefore adjusted at 25 minutes. In Figure 16, the data starts when the LN_2 was turned on. The simulator was not turned on until a reasonably low wall temperature was reached at 50 minutes. This delay is not represented in the analysis. All other data points fall within the usual 10°F uncertainty band.

As previously mentioned, the solar simulator was not adjusted correctly resulting in a spectral red shift of the incident energy. This was first noticed when an I-V curve was measured on the IR transparent module A, but was not explained until detailed data analysis was initiated. Four data points were taken using a resistive load. At each data point, the sample was allowed to reach thermal equilibrium. A smooth curve was plotted through these data to extrapolate the value of I_{sc}. A comparison of pretest and test electrical measurements showed an 11% reduction in I_{sc}, Figure 23. When combined with the data from the black plate radiometer, which is spectrally insensitive, the existence of the red shift was verified.

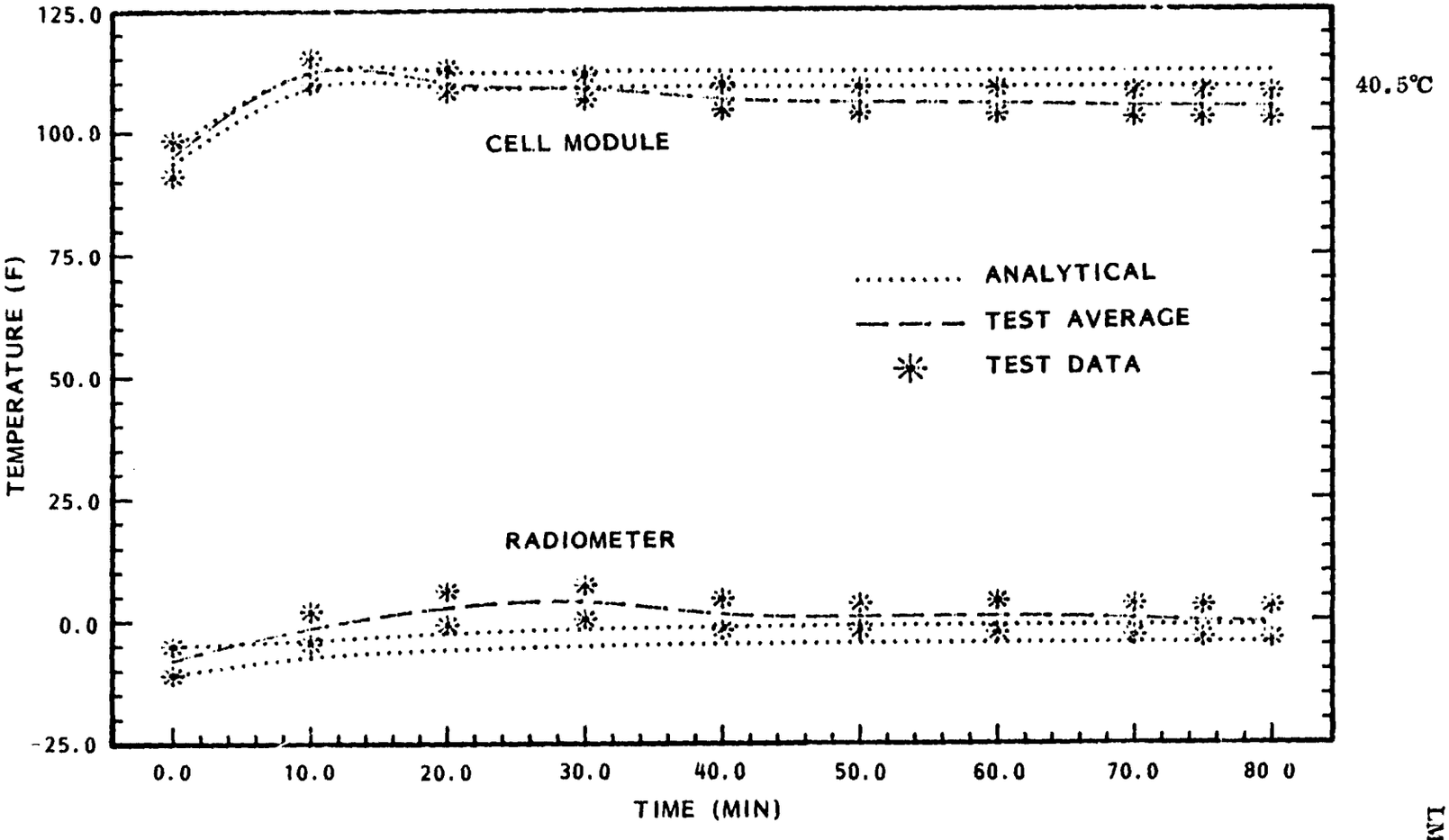

Figure 13 Module A (137.2 mW/cm^2) - Temperature vs Time

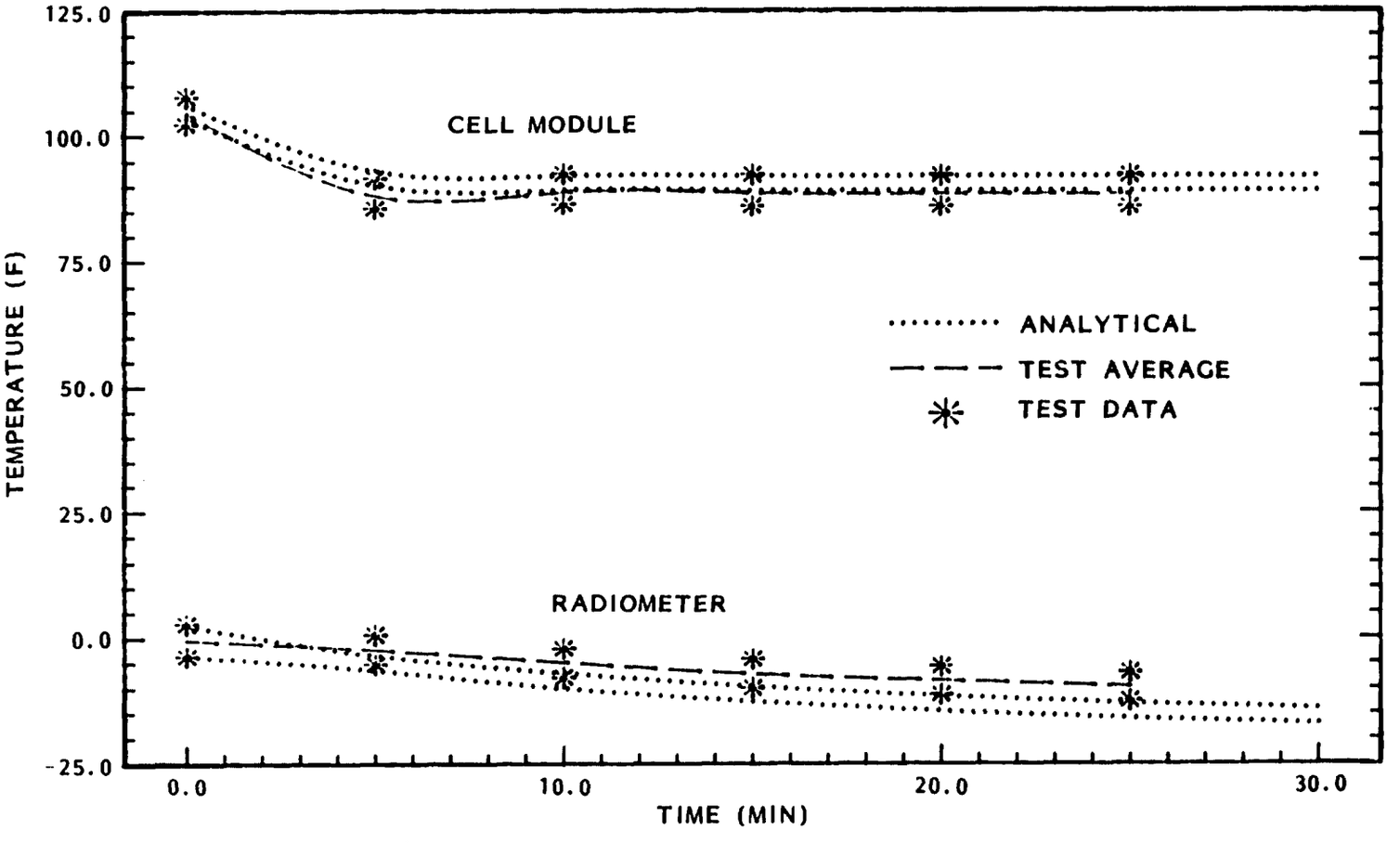

Figure 14 Module A (129.3 mW/cm^2) - Temperature vs Time

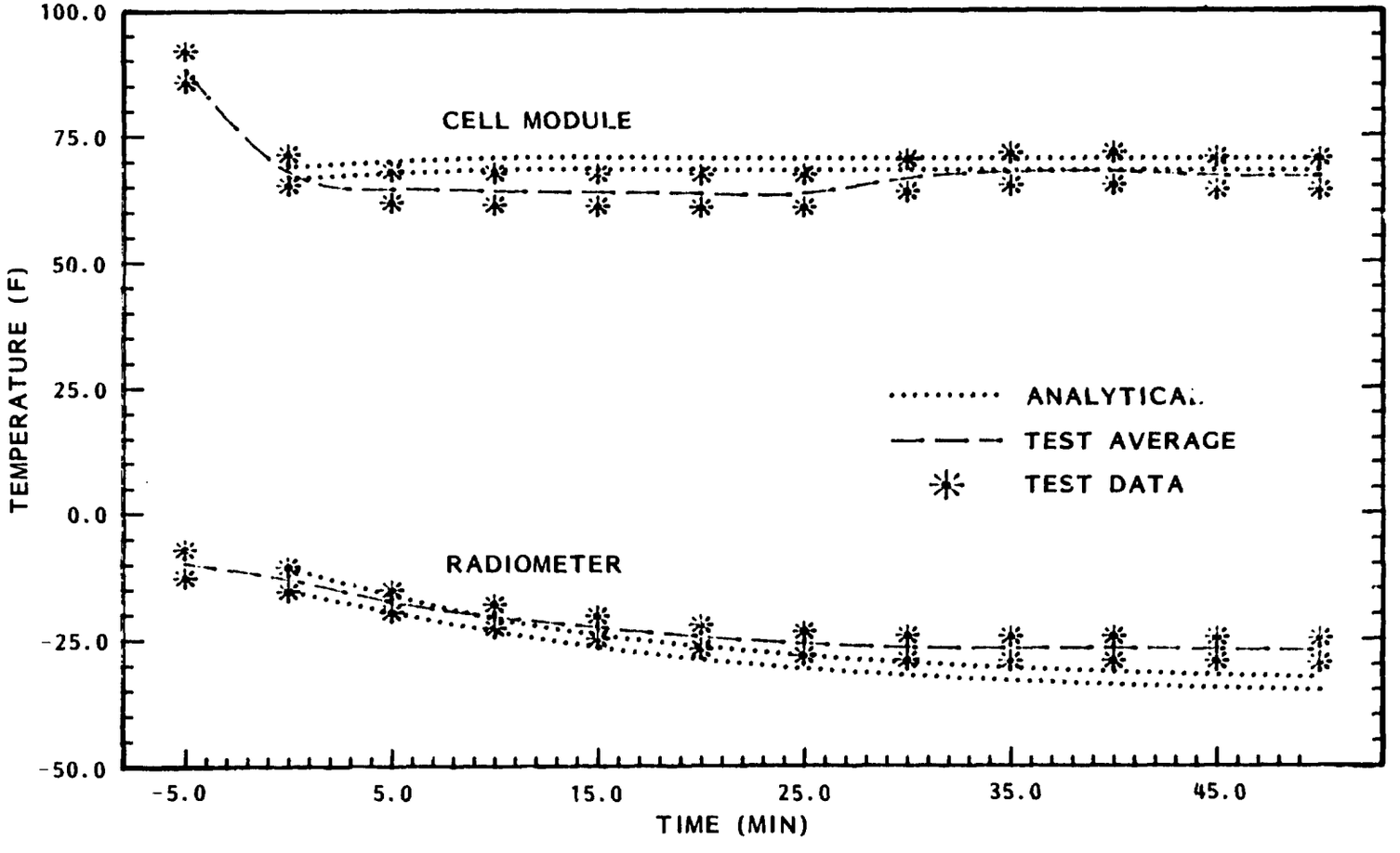

Figure 15 Module A (101.2 mW/cm^2) - Temperature vs Time

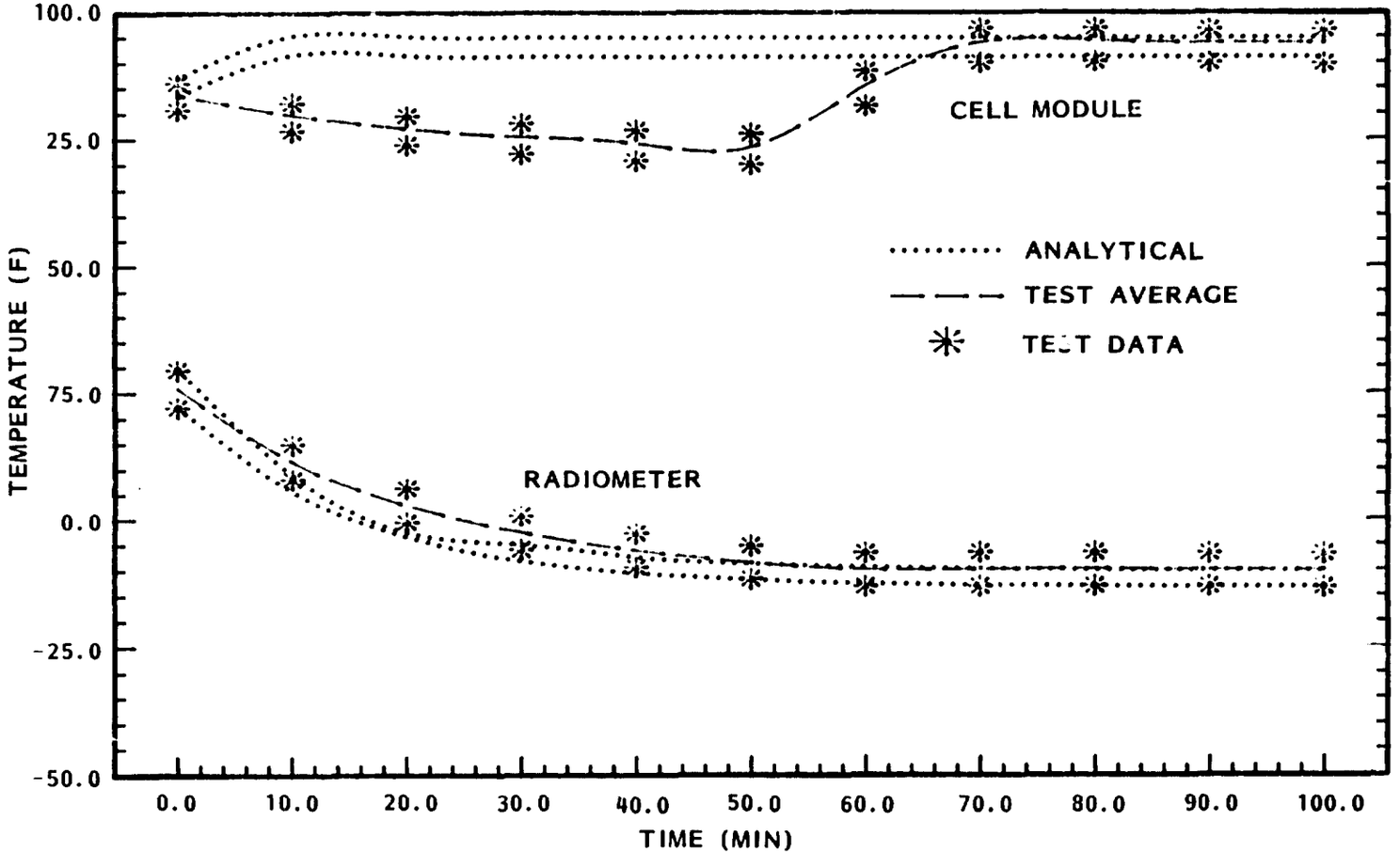

Figure 16 Module B (137.2 mW/cm^2) - Temperature vs Time

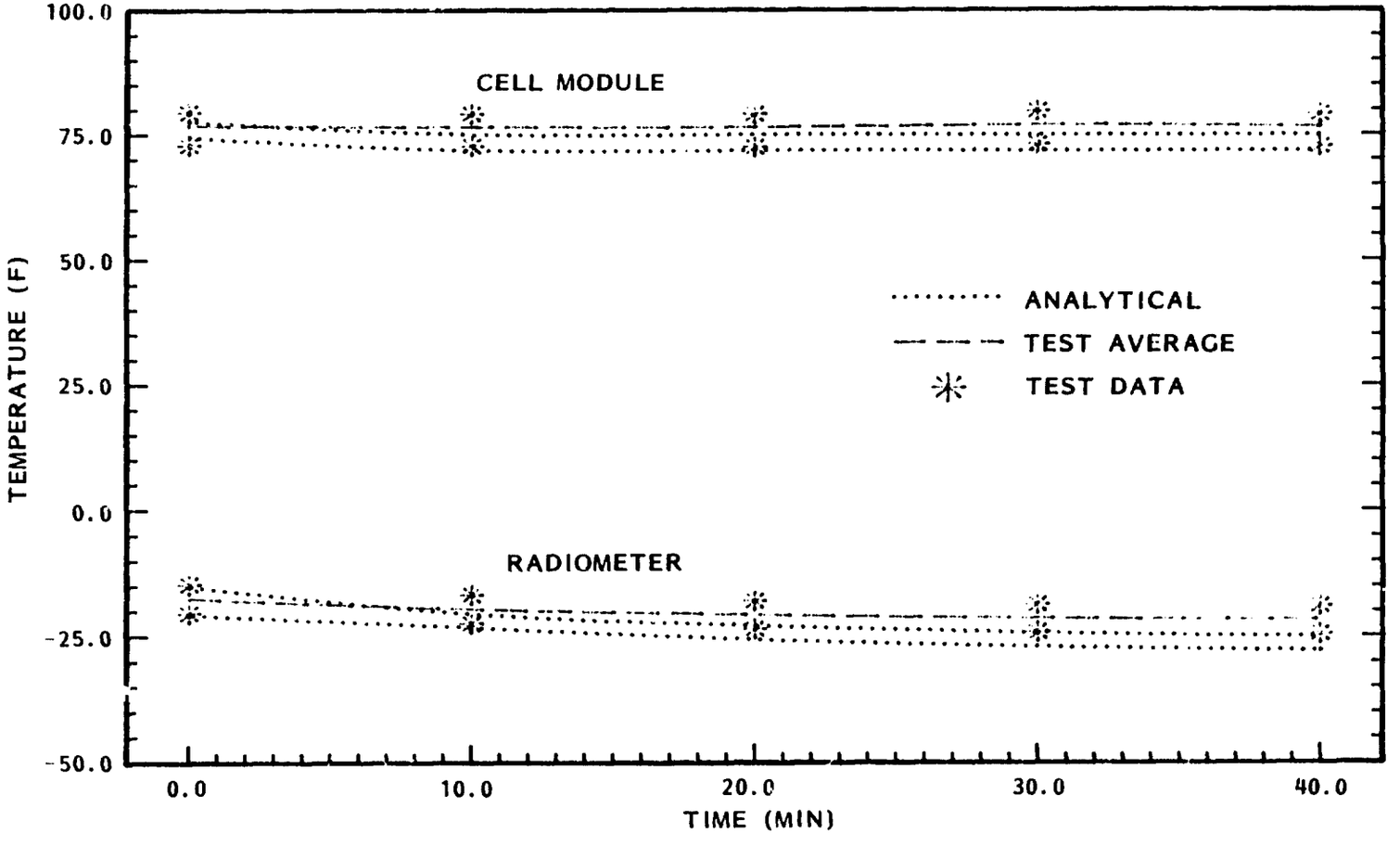

Figure 17 Module B (129.3 mW/cm^2) - Temperature vs Time

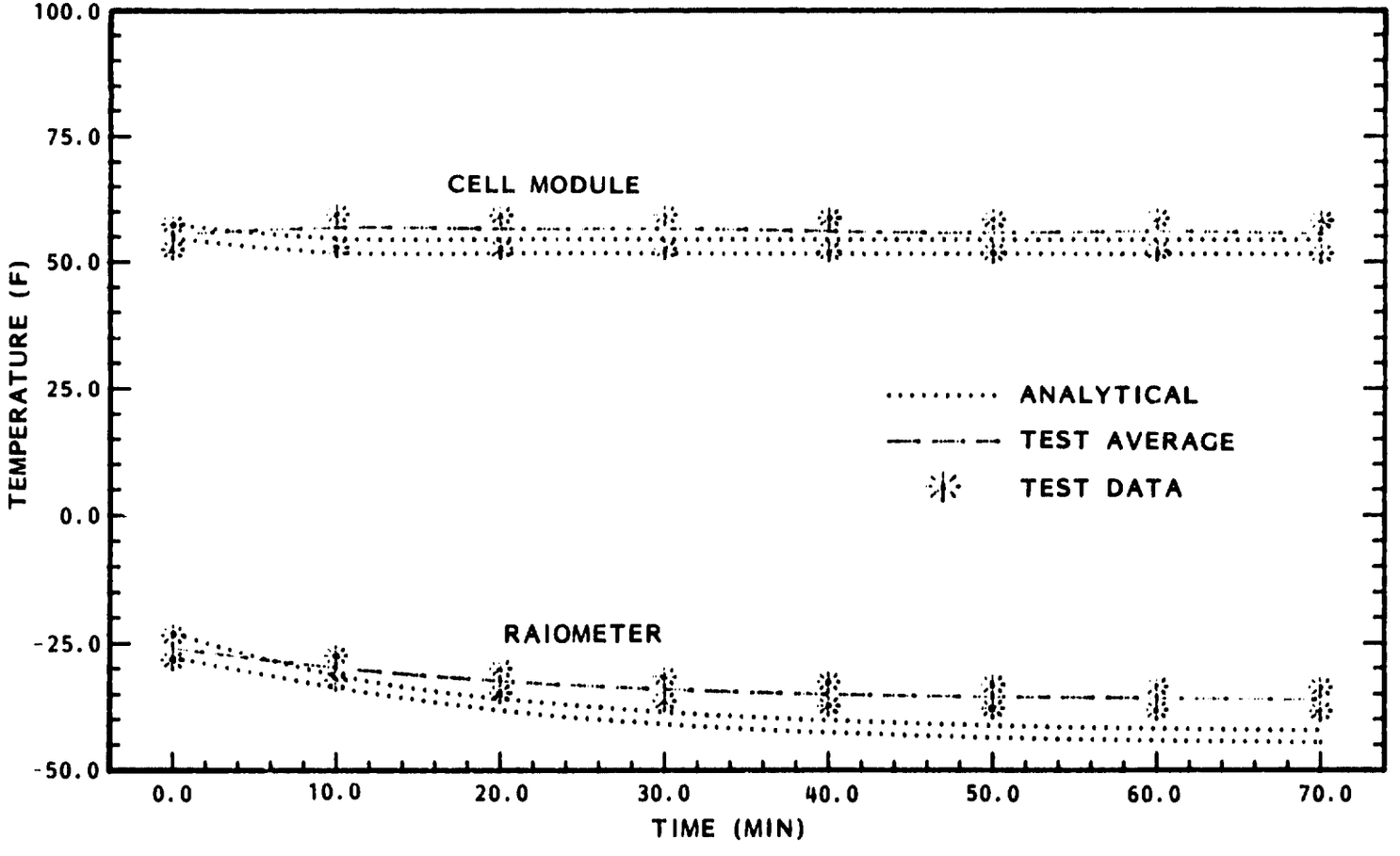

Figure 18 Module B (101.2 mW/cm^2) - Temperature vs Time

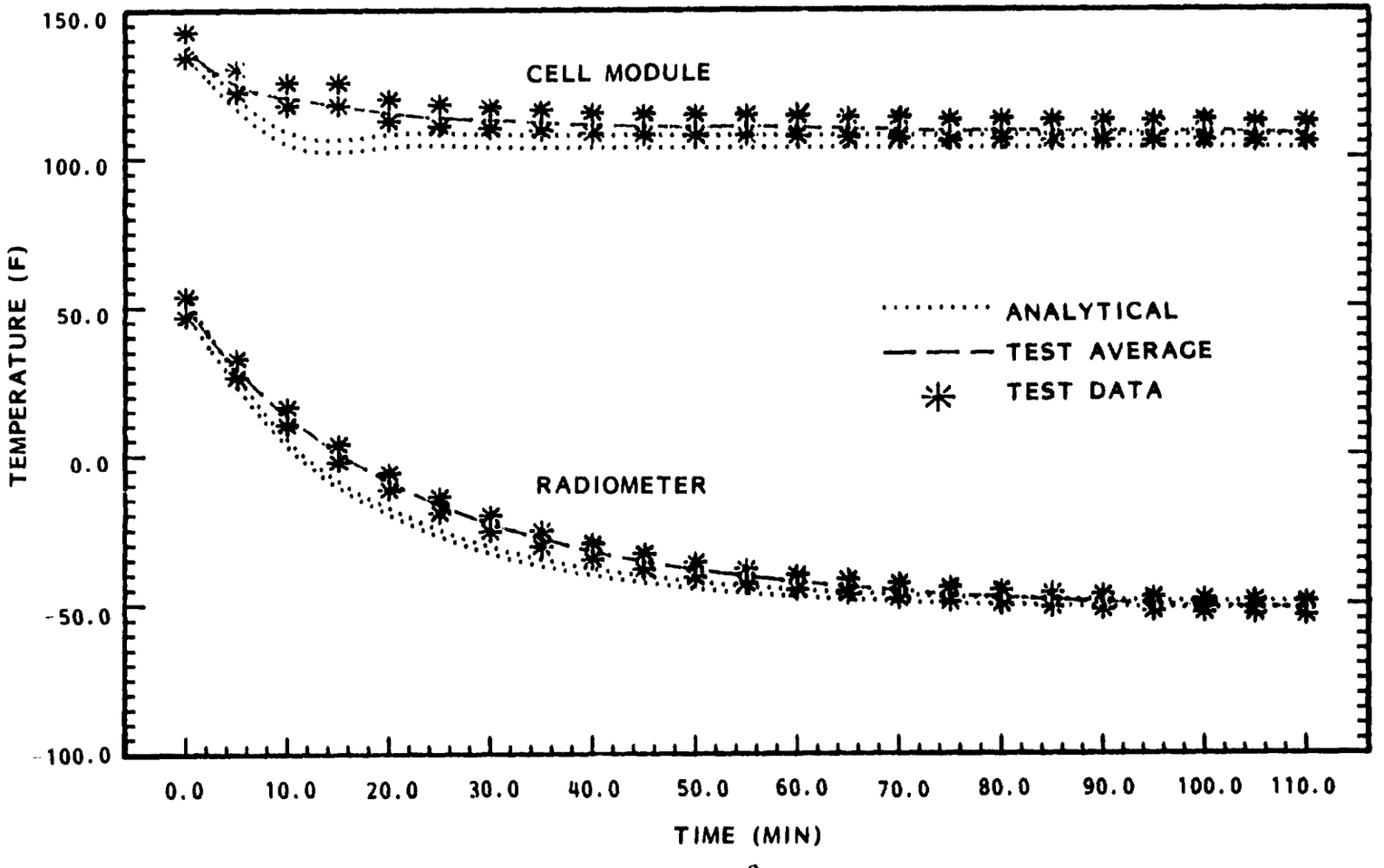

Figure 19 Module C (137.2 mW/cm^2) - Temperature vs Time

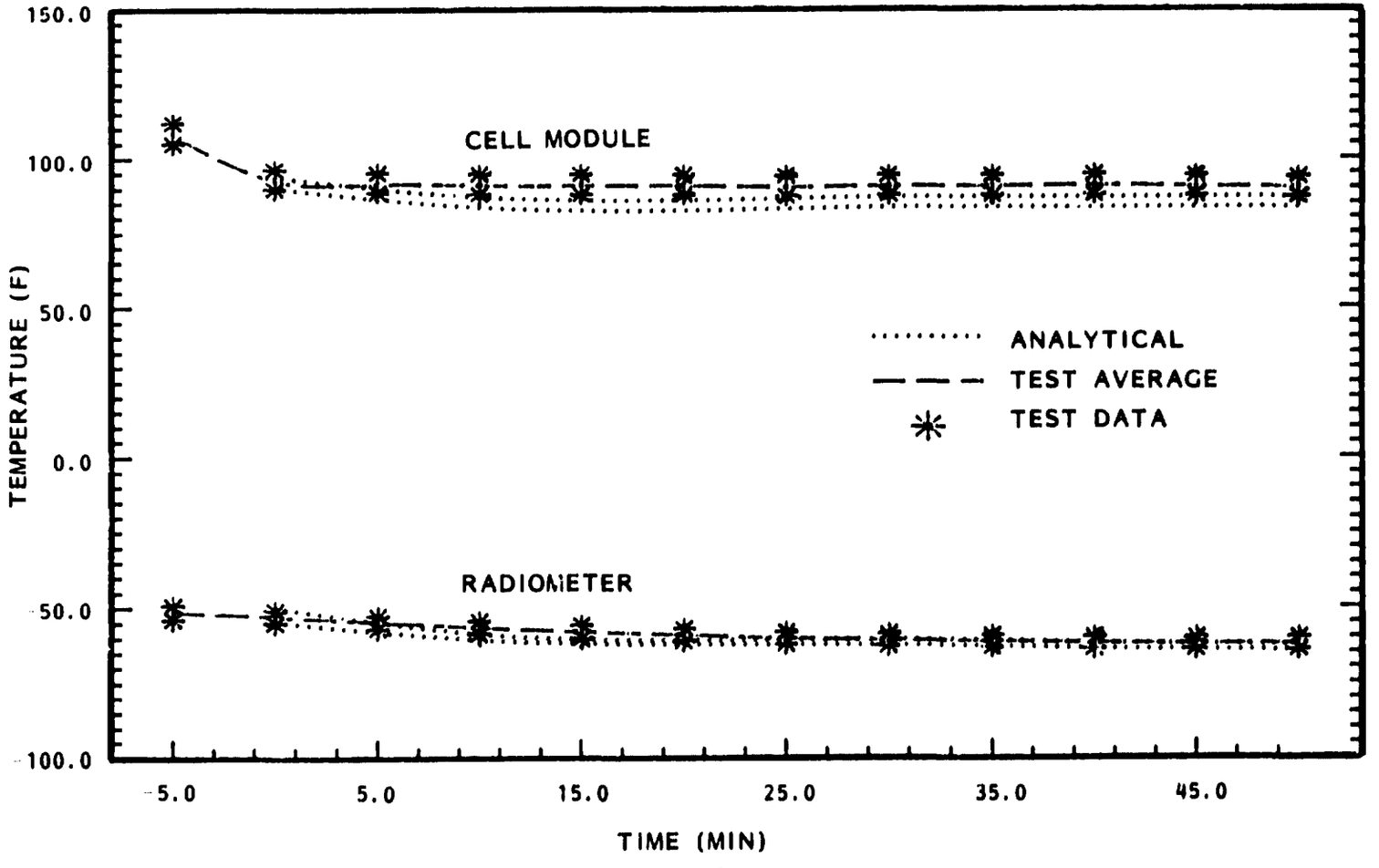

Figure 20 Module C (129.3 mW/cm^2) - Temperature vs Time

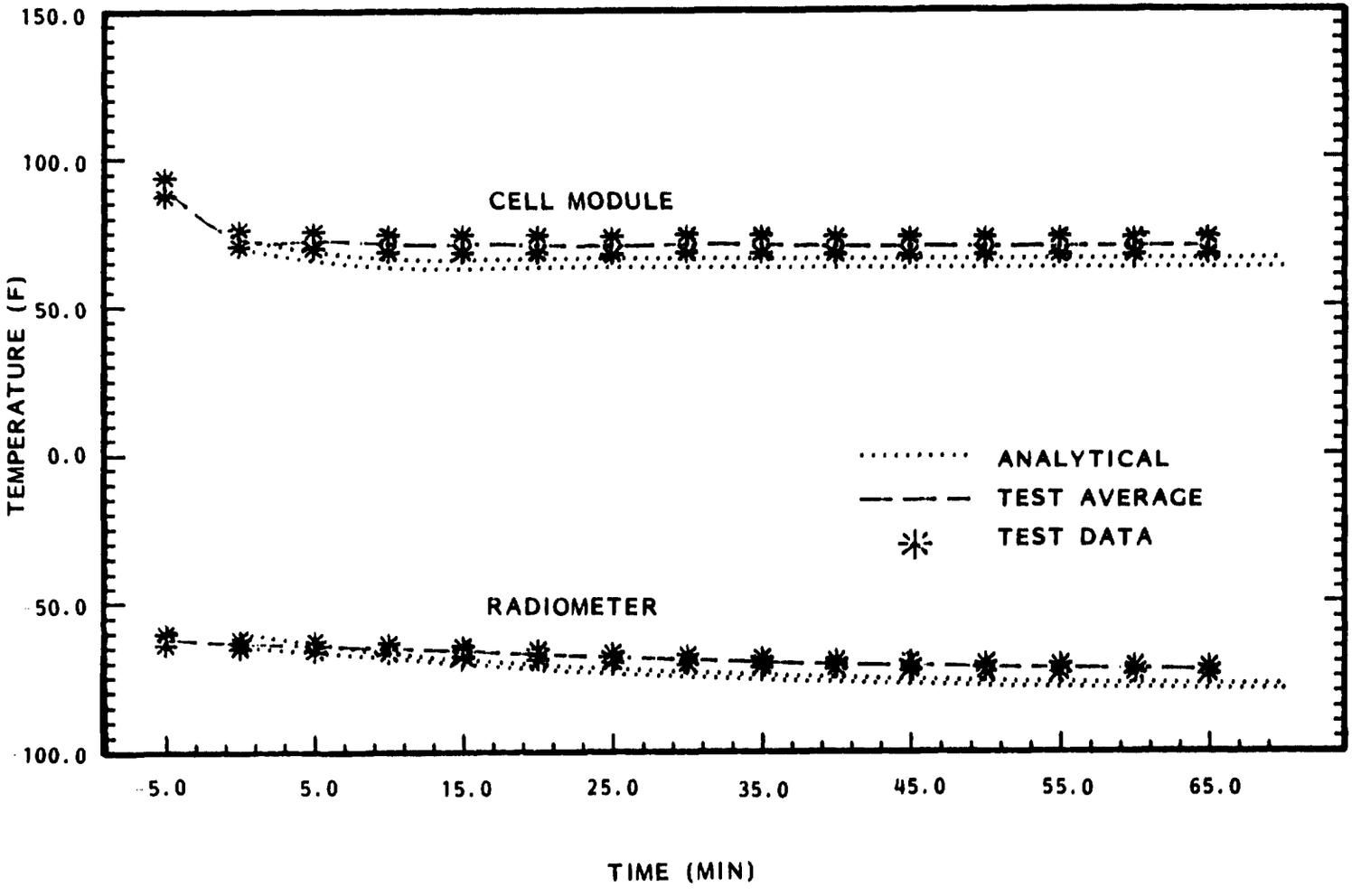

Figure 21 Module C (101.2 mW/cm^2) - Temperature vs Time

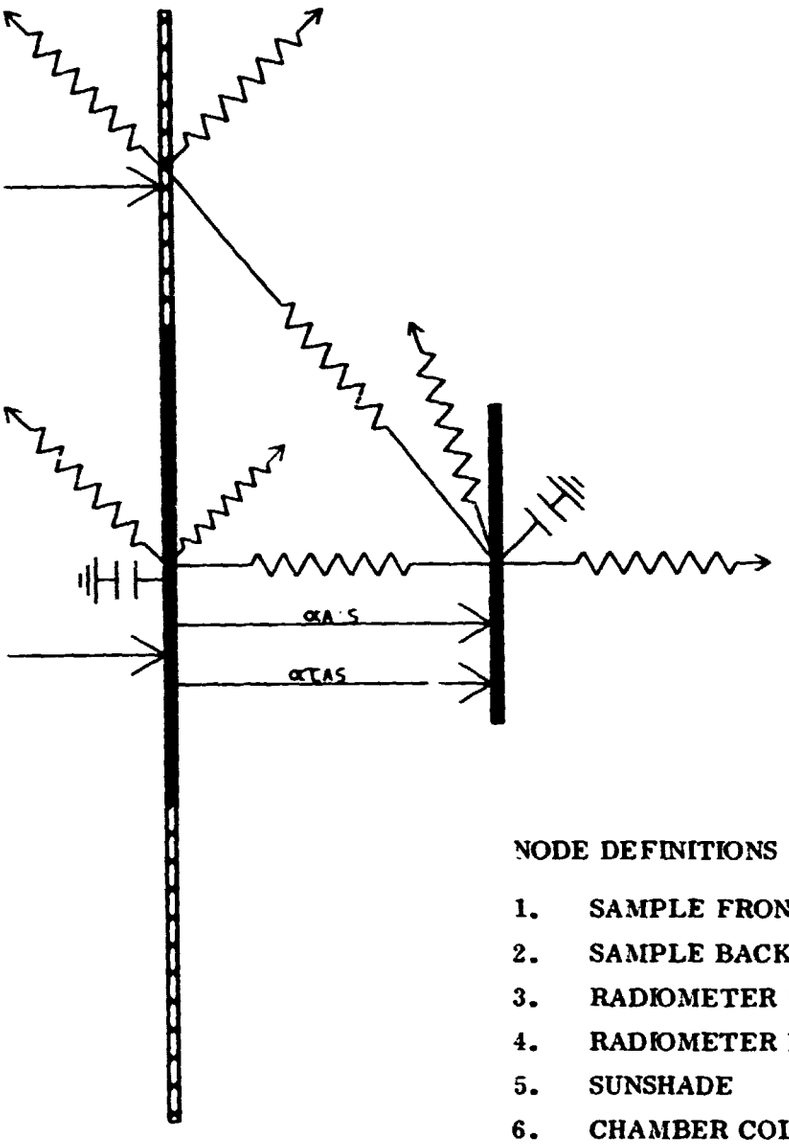

NODE DEFINITIONS

1. SAMPLE FRONT
2. SAMPLE BACK
3. RADIOMETER FRONT
4. RADIOMETER BACK
5. SUNSHADE
6. CHAMBER COLD WALLS

Figure 22 Thermal Analysis Model

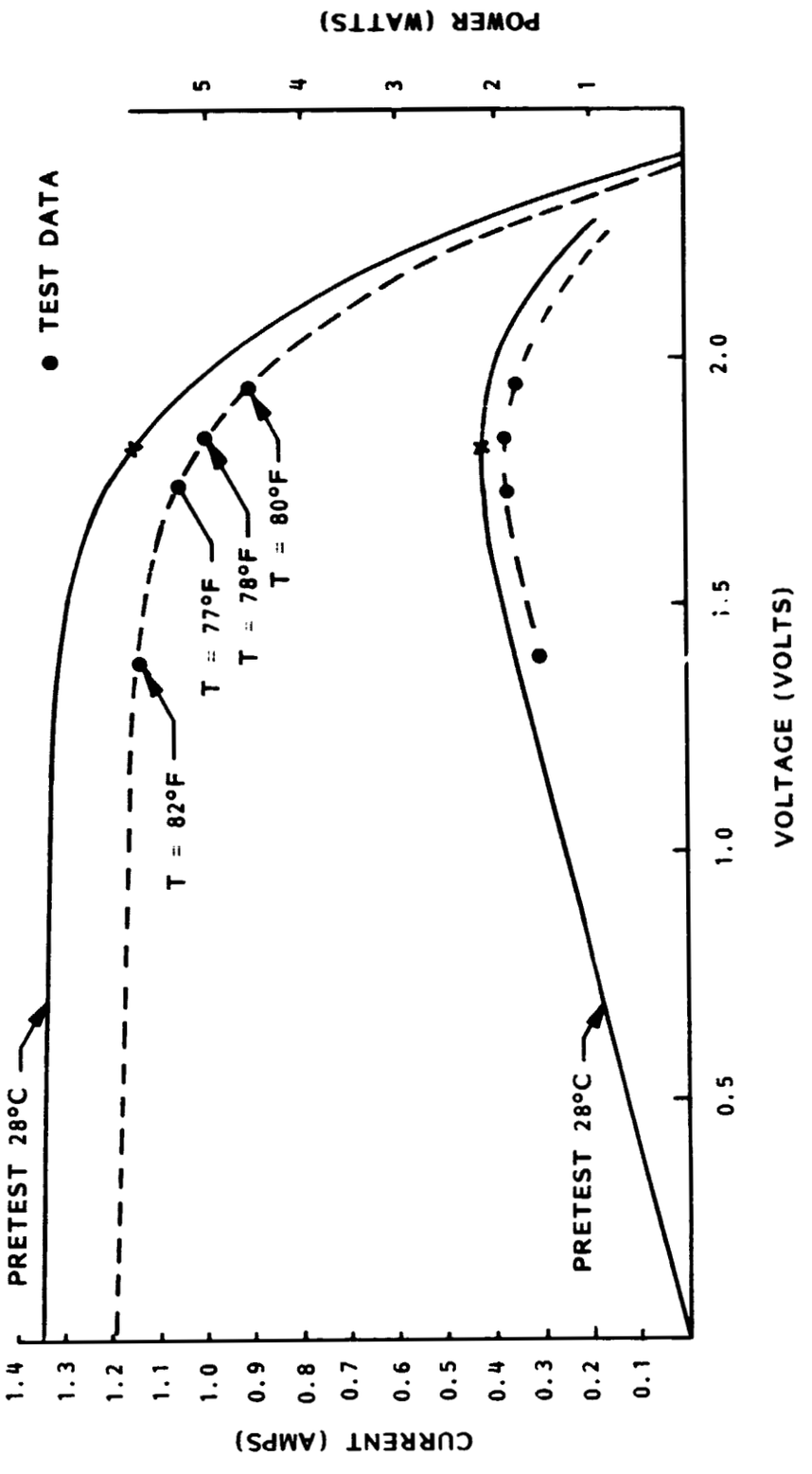

Figure 23 Panel A Electrical Characteristics

In order to evaluate the effects of this spectral shifting on the test results, a simple analysis was undertaken. The solar absorptance of a solar cell can be represented as an integration over three spectral regions, i.e.,

$$\alpha = \frac{\int_0^{0.35} \alpha_\lambda S_\lambda \, d_\lambda + \int_{0.35}^{1.1} \alpha_\lambda S_\lambda \, d_\lambda + \int_{1.1}^{4.0} \alpha_\lambda S_\lambda \, d_\lambda}{\int_0^{\infty} S_\lambda \, d_\lambda}$$

For all of the test samples being considered, a UV reflecting filter was applied to the cover rendering the first term very small. In addition, in the third term, α_λ is small either because of transparency or reflection. It is therefore clear that for relatively small spectral shifts in the intensity distribution function, S_λ, the primary effects on α are due to the $0.35 \leq \lambda \leq 1.1\,\mu$ spectral region. By examining the details of the absorptance spectra over this band, the absorptance is seen to be relatively constant. This allows us to compare the effect on absorptance as:

$$\frac{\alpha_1}{\alpha_2} = \frac{\int_{0.35}^{1.1} S_1(\lambda) \, d_\lambda}{\int_{0.35}^{1.1} S_2(\lambda) \, d_\lambda}$$

This spectral region is also where the electrical conversion process takes place. The measured short circuit current, I_{sc}, can be formulated in terms of the incident spectral distribution function as follows:

$$I_{sc} = \int_{0.35}^{1.1} I_{sc}(\lambda) \, S(\lambda) \, d_\lambda$$

where $I_{sc}(\lambda)$ is the spectral response of the device. If the spectral shift is small, an average value of $I_{sc}(\lambda)$ over the integral can be used and brought outside of the integral. In this case, the effect of the shift can be evaluated by comparing the I_{sc} for each spectral distribution, i.e.,

$$\frac{I_{sc(1)}}{I_{sc(2)}} = \frac{\int_{0.35}^{1.1} S_1(\lambda) \, d_\lambda}{\int_{0.35}^{1.1} S_2(\lambda) \, d_\lambda}$$

With this result we can now substitute the measured values for I_{sc} under the two spectra and calculate the reduced absorptance due to the shifted spectra:

$$\alpha_1 = \frac{I_{sc(1)}}{I_{sc(2)}} \times \alpha_2$$

This method provides results which agree very closely with the measured thermal data.

Section 6
CONCLUSIONS AND RECOMMENDATIONS

As a result of this test program, we have verified an analytical model showing that a significant degree of IR transparency can be designed into a flexible solar array. Test data correlates with both steady state and transient thermal analyses.

The analysis was extended to predict the orbital performance of a solar array incorporating IR transparency. For the purpose of the comparison presented here, questions concerning packing factors, cell mismatch, UV loss and other design specific parameters was sidestepped by comparing only cell orbital efficiency.

The Solar Array Experiment (SAE) was chosen as the baseline design. Data from a series of thermal balance tests on SAE development units showed that the specified 12.5% (at 28°C) efficient cells (2 ohm-cm, BSR, $\alpha = 0.70$) would operate at 59°C and 10.9% efficiency in a GEO type orbit. Advances in cell processing have increased the basic efficiency to 13.5% (at 28°C). Directly substituting this cell into the SAE design under the same conditions leads to a predicted operating point at 58°C and 11.8% efficiency. This latter condition will be used in our comparison.

For the basic IR transparent array, measured cell properties from several different batches were used. From this data base, we believe that a conservative cell specification of $\alpha = 0.64$ with an efficiency of 13.5% (at 28°C) is achievable. Using the validated model from this series of tests, under the same operating conditions as the SAE baseline results in a predicted operating point of 17.9°C and 14.1% efficiency. This is an increase of 19.49% in power by reducing temperature 40°C.

Additional improvements in thermal design are possible with minimal development. Projecting the cell and array thermo-optical properties to those currently believed achievable results in a 4.1°C operating temperature with an efficiency of 14.85%. By making assumptions about design specific variables based upon either experience or analysis, the expected power density for a silicon advanced planar array is 172 W/m^2.

Recommendations for future effort are centered about a five year plan to integrate recent technology development programs into a demonstration flight qualified unit. The proposed system design should be targeted at GEO and interplanetary missions which require the very lightweight, high performance provided by a flexible, IR transparent array.

Section 7
NEW TECHNOLOGY

No new technology was developed during this contract.

APPENDIX A

MATERIAL PROPERTIES

MATERIAL PROPERTIES

A literature search and review of the LMSC data base on thermo-optical properties was completed with mixed results. Standard sources for material property data, including the Handbook of Optics by McGraw-Hill and Thermophysical Properties of Selected Aerospace Materials edited by Y. S. Touloukian and D. T. Ho, were consulted for data on materials of interest. Where data was available on materials being considered, the spectra given had large amounts of scatter, presumably owing to variations in sample formulation.

Previous measurements at LMSC were made with a normally incident beam and a detector with a narrow, ~5°, field of view. This type of measurement technique can provide qualitative data on the spectral content of the transmitted beam but is subject to large errors if the sample scatters the beam.

As a result of the materials property data review, it was determined that an alternate testing method was desired to get accurate, quantitative spectral data on scattering materials. Two techniques were deemed feasible. The most accurate results would be obtained by inserting an integrating sphere into the optical path between the sample and detector and directly measuring the total hemispherical transmittance. Unfortunately, this particular approach would require a new detector with at least an order of magnitude more sensitivity and probably photon counting techniques with large integrating times. Cost and schedule constraints therefore eliminated this technique.

The second technique which was pursued involved using bandpass filters, a more intense illumination source, and an integrating sphere and detector from an alternate instrument. This technique would provide the required intensity at the expense of a loss in spectral quality and continuity. Bandpass filters are commercially available to approximately span the range of interest in 0.5μ steps. The feasibility of implementing this approach was investigated with the research

staff at PARL. Though it appeared this technique would be applicable, the general consensus was a one year program involving a senior staff member. This was clearly outside the scope of this contract. Therefore, the spectra included in this appendix were made on a Cary 14 for $\lambda<1.8\mu$ using an integrating type detector, a Perkin-Elmer Spectrometer with a 5° FOV for transmittance with $\lambda>1.1\mu$ and a Gier-Dunkle heated Hohlraum for reflectance for $\lambda>1.1\mu$.

MEASURED SPECTRAL PROPERTIES LIST

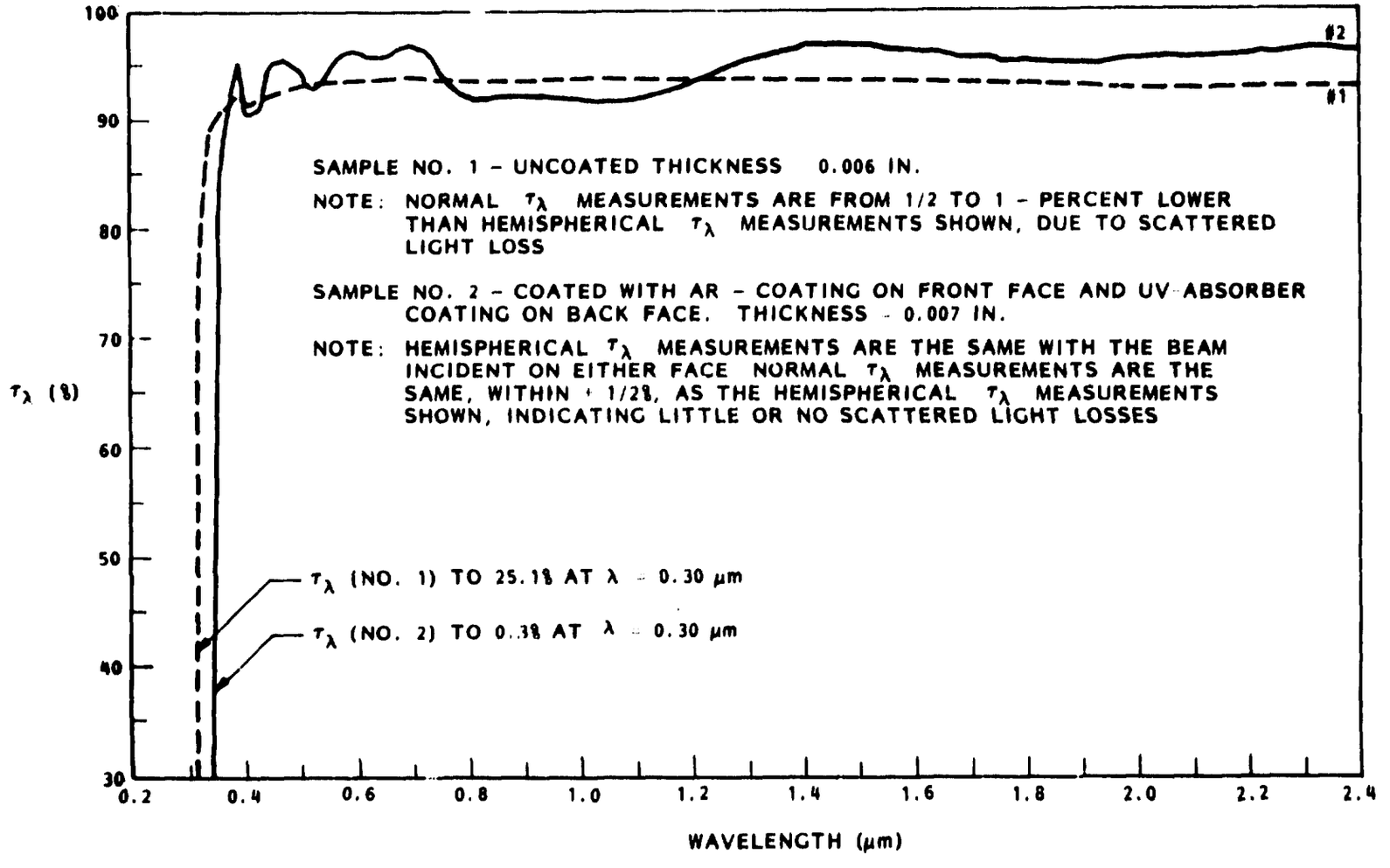

Figure 1 Spectral Transmittance Data for Coated and Uncoated Microsheet Samples

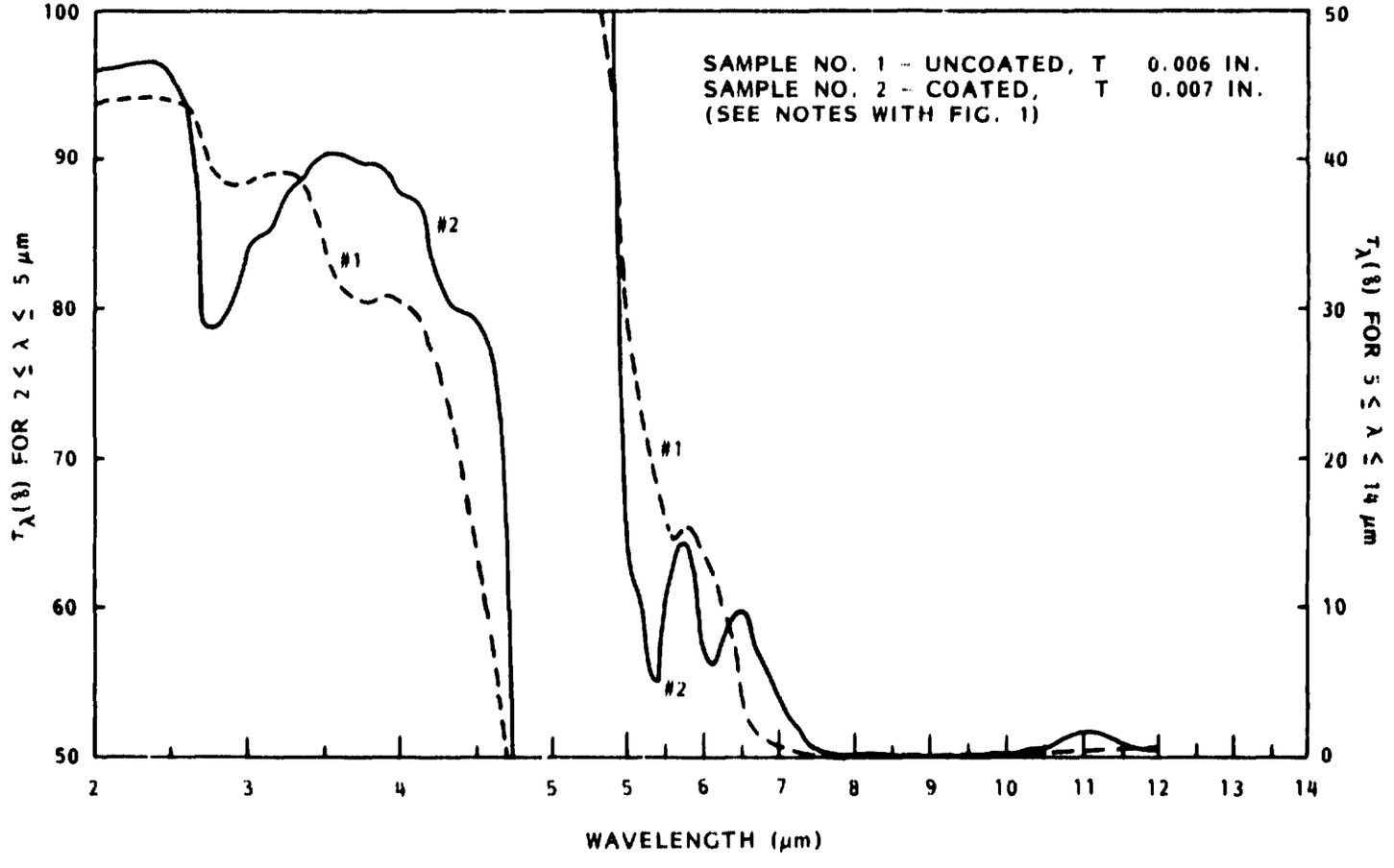

Figure 2 Spectral Transmittance Data for Coated and Uncoated Microsheet Samples

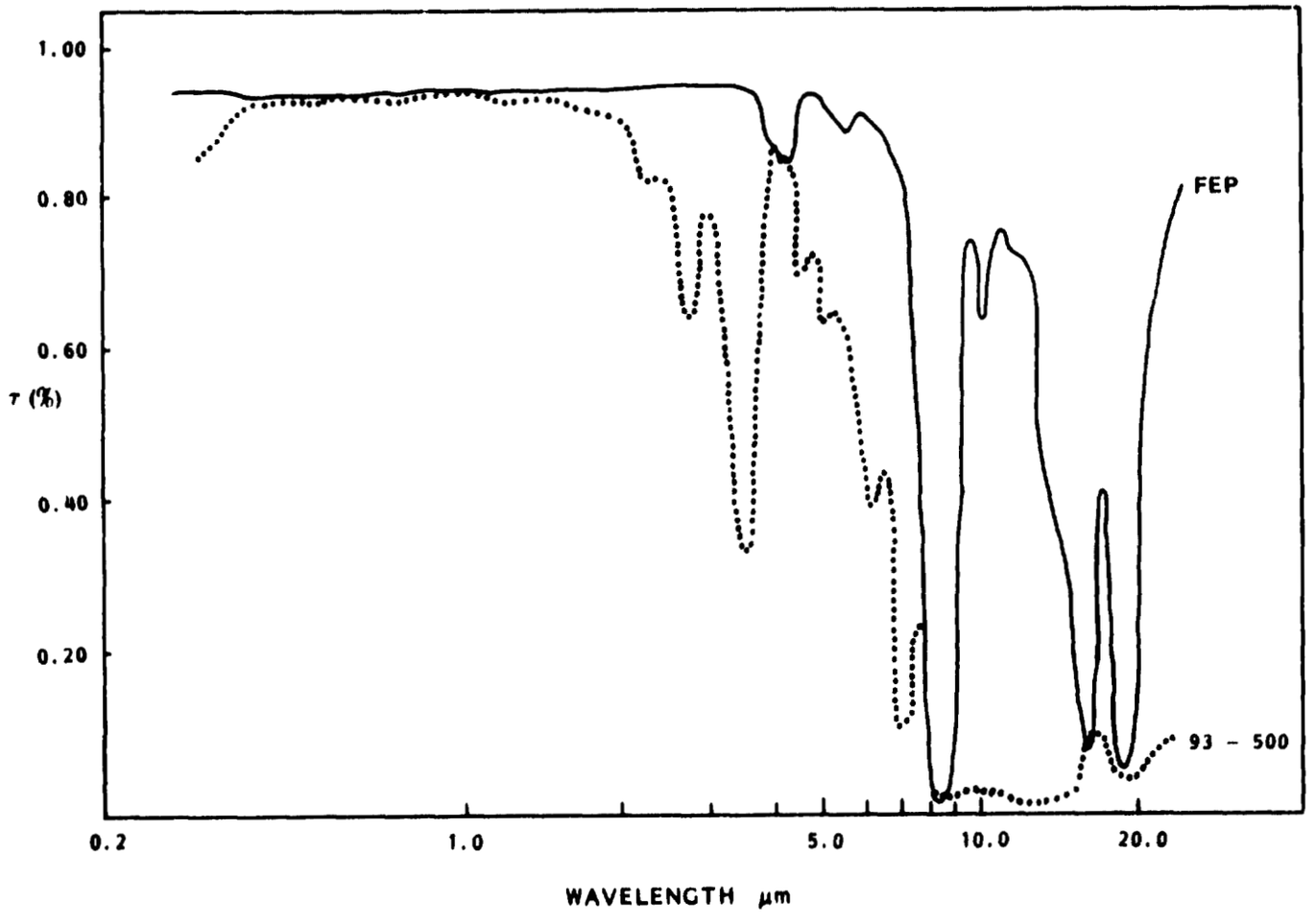

Figure 3 Transmittance Comparison FEP Versus DC93-500

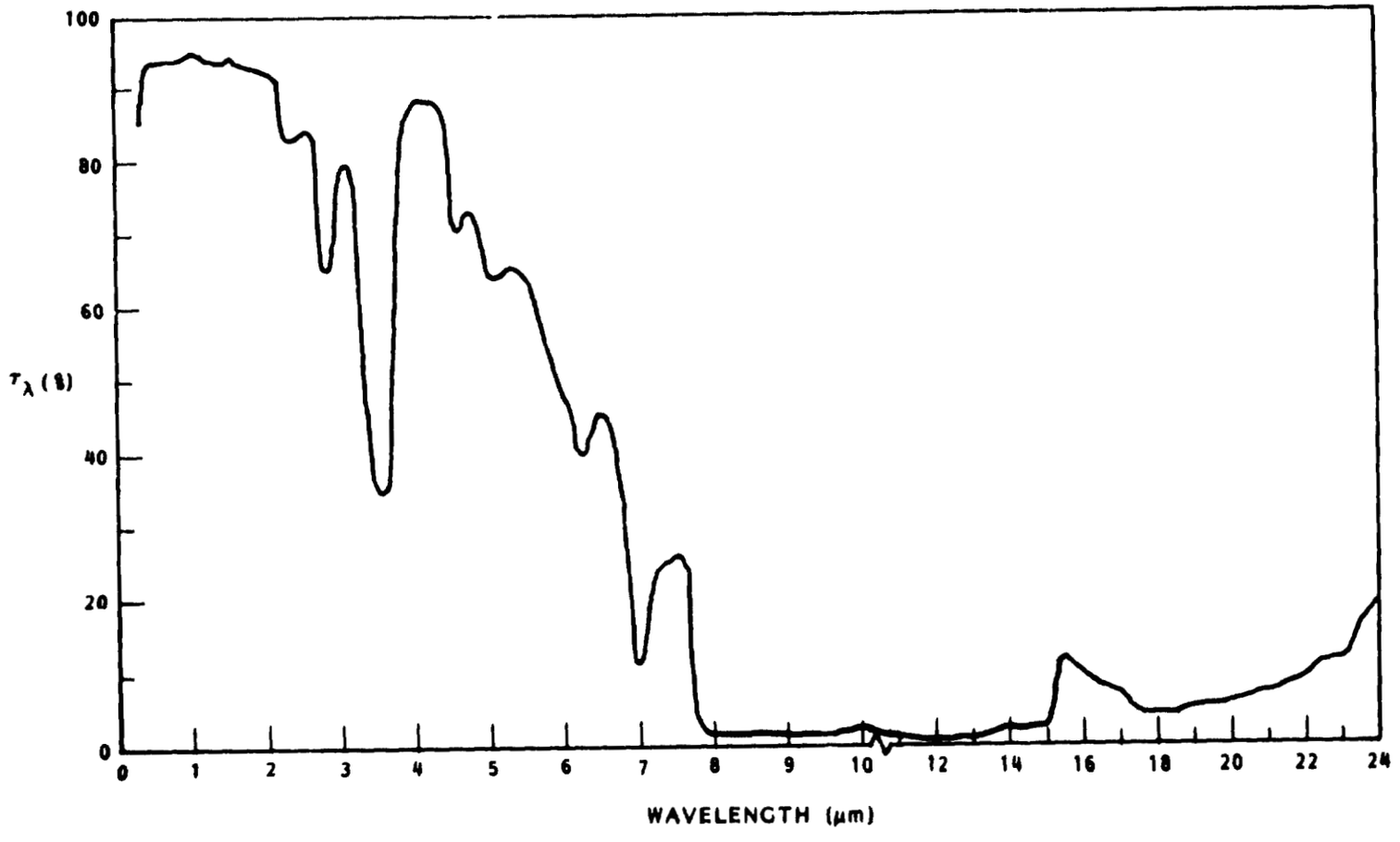

Figure 4 Spectral Transmittance Data for a 0.005 Inch Film of DC93-500

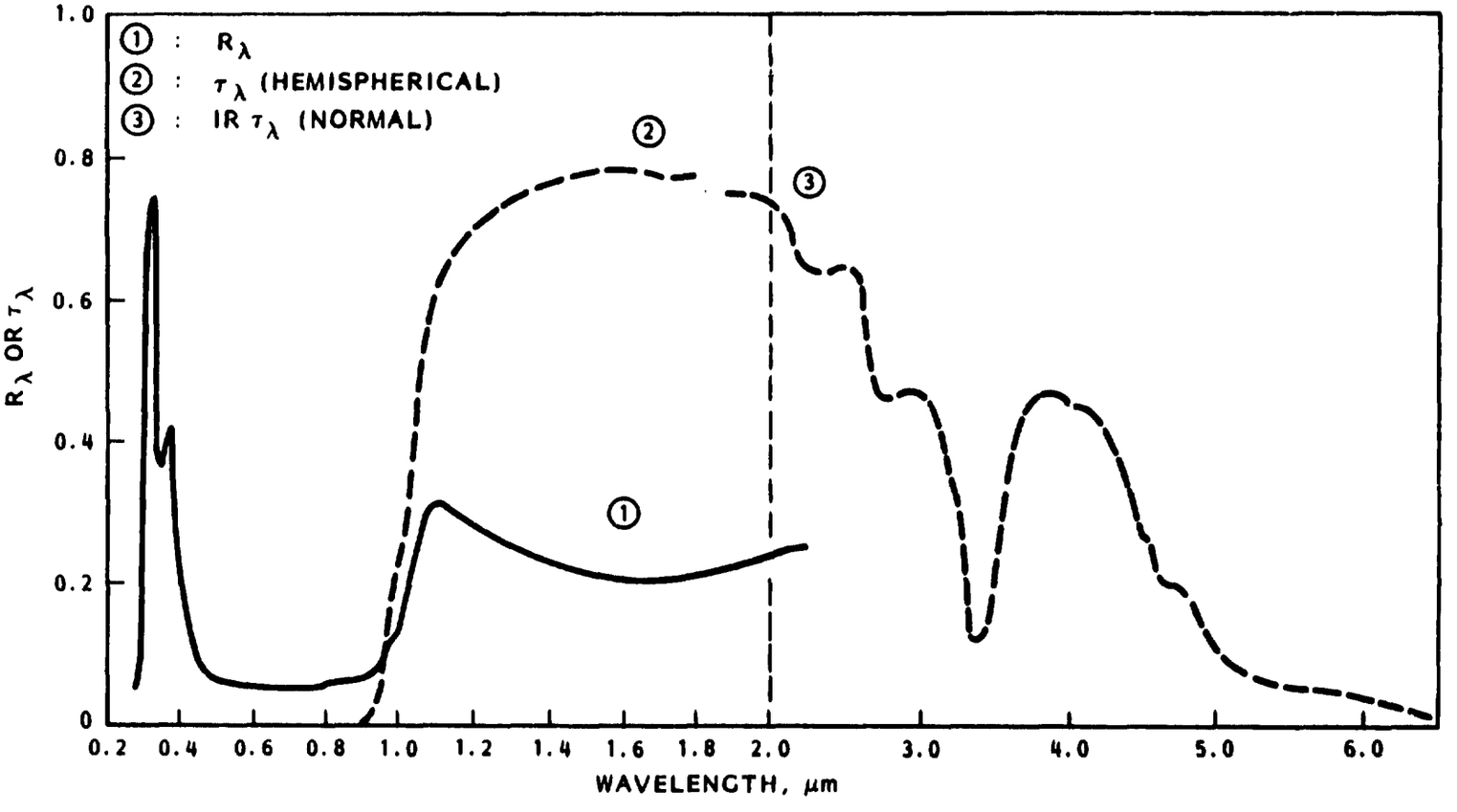

Figure 5 Spectral Reflectance and Transmittance Data for Solar Cell Sample #AG-3

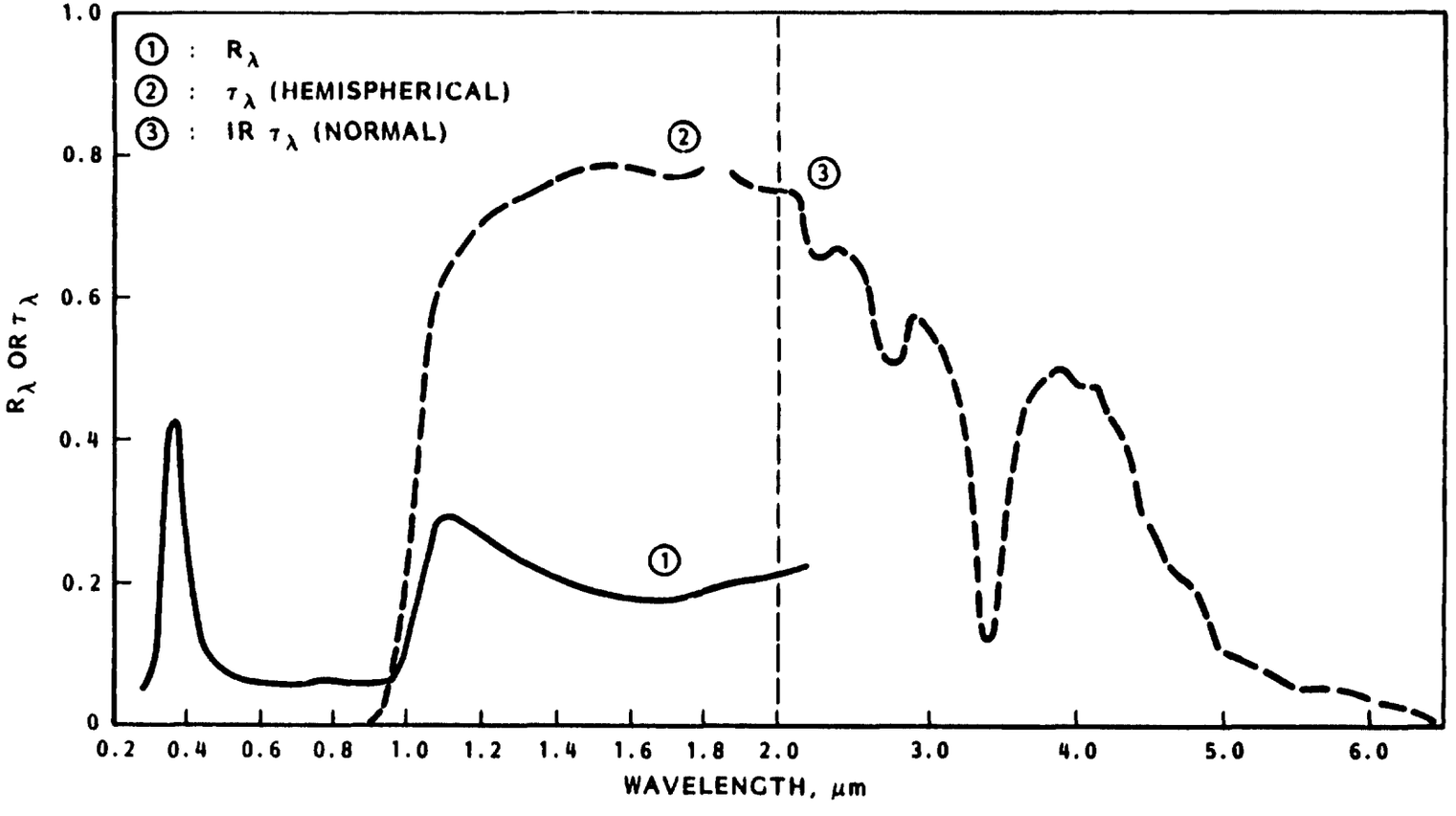

Figure 6 Spectral Reflectance and Transmittance Data for Solar Cell Sample #AG-20

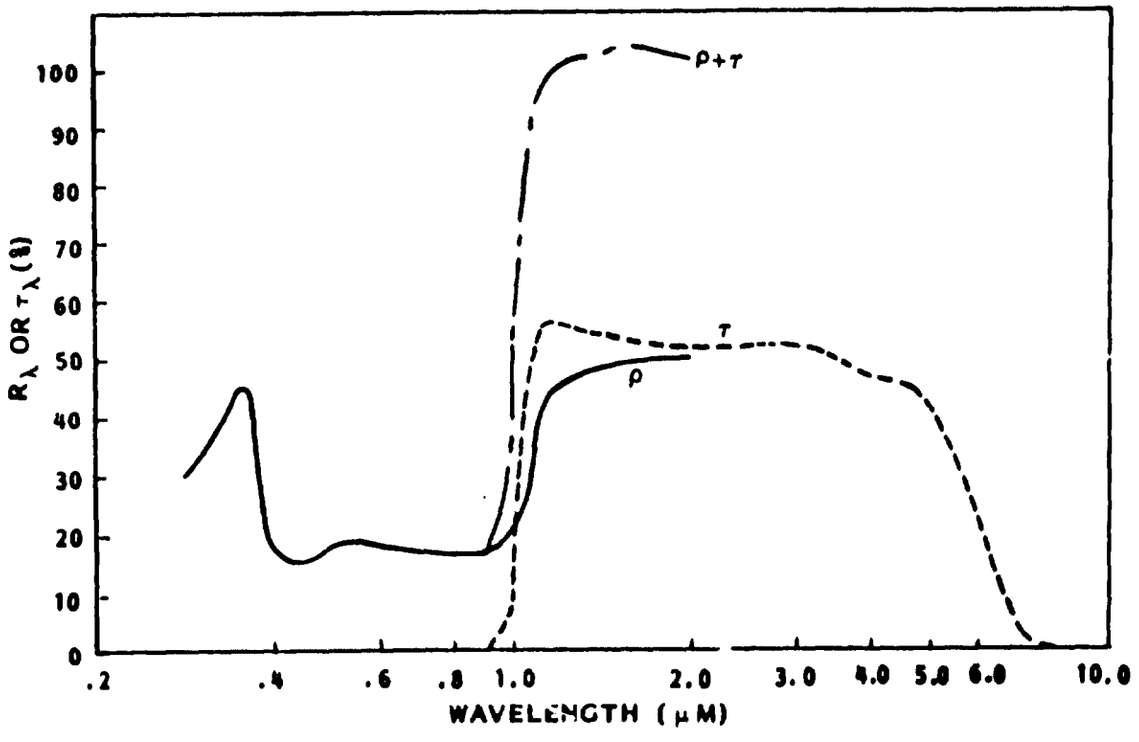

Figure 7 Typical Spectral Reflectance and Transmittance for a Gridded Back Contact Cell Without AR Coating

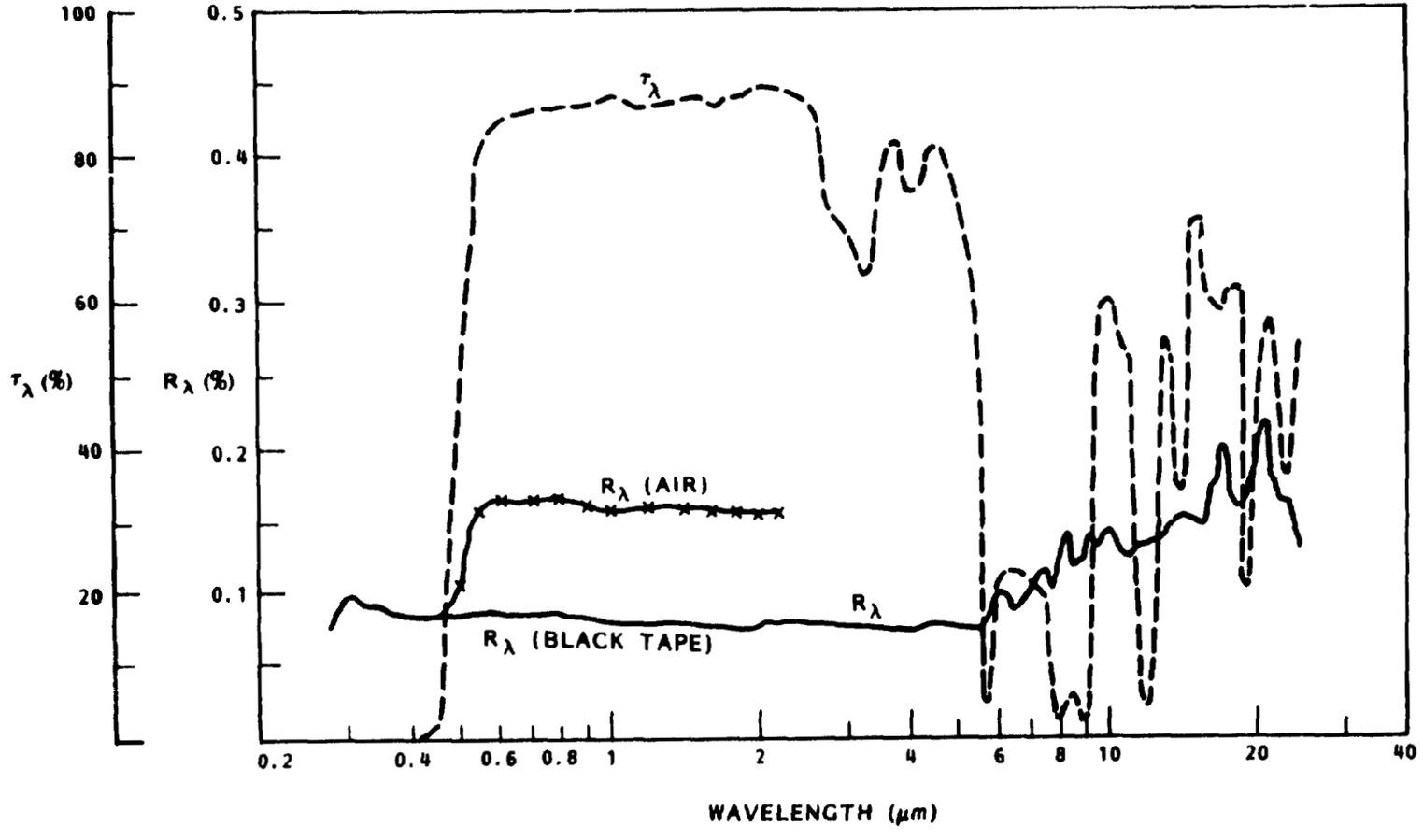

Figure 8 Spectral Reflectance and Transmittance Data for a 0.001 Inch Kapton Film

APPENDIX B
TEST PLAN

TEST PLAN

DEMONSTRATION OF
TRANSPARENT SOLAR ARRAY MODULE DESIGN

JPL Contract 956608

Prepared by: _____
J. Lilly
Electrical Power Systems

Approved by: _____
G. J. Pack
Electrical Power Systems

1.0 INTRODUCTION

This report details facility conditions and procedures for a thermal balance test of IR transparent solar array modules as required by JPL Contract No. 956608. The goal of this test is to verify by experiment the analytical predictions of reduced operating temperature due to substantial IR transmission.

1.1 TEST CONDITIONS SUMMARY

Number of Test Modules

(1) Module A Baseline Without Transparent Components
(1) Module B Conceptual Transparent
(1) Module C Enhanced Transparent

Instrumentation

Thermocouple Channels	32

Vacuum Chamber

Wall Temperature	-300°F
Vacuum Pressure	1×10^{-4} Torr

2.0 TEST FACILITY AND TEST CONDITIONS

2.1 DESCRIPTION OF TEST CHAMBER

Ultek Temperature Vacuum Chamber designated as #14 with reference tag number LMSC 88035. This chamber is classified class "B" and conforms to the criteria established for this class of equipment.

2.2 FEATURES

- The Ultek chamber has a liquid nitrogen shroud (approximately 57.0 inches in diameter by 71.0 inches) which can permit specimen cooling to approximately -300°F.

- All surfaces exposed to the inside except where penetrations are required for solar simulation, pass-throughs, etc. are painted with a black high emissivity coating giving an emittance of approximately 0.95.

- R/I controllers can be programmed for heat flux input.

- Roughing system consiting of a mechanical pump, blower and liquid-nitrogen cold tap.

- Fine pumping is accomplished by a Ultek ion pump.

- With all pumping systems operating and the shrouds cold, the system is capable of reaching a pressure of 1×10^{-10} torr in 24 hours. During simulation testing, the required pump down time is 2 to 3 hours.

- An 8 inch-diameter ultra-violet grade quartz window is provided at one side of the chamber wall through which a beam of spectrally matched solar radiation can be passed into the chamber and on to the test specimen.

- The system pressure is monitored by two vacuum gauges. The liquid-nitrogen shroud temperatures are to be monitored with 7 copper-constantan type thermocouples.

3.0 TEST PLAN

3.1 For the thermal balance solar array transparent test, Engineering (62-16) will supply solar cells 5.9 x 5.9 cm gridded back cells in at least a 4-cell module. The total test matrix will be as follows:

- Module A Baseline Module without transparent components (SAFE design)
- Module B Conceptual Transparent
- Module C Enhanced Transparent

3.2 Intensity profiles of sun simulator lamp (Spectrolab X-25L) shall be run prior to and subsequent to all thermal cycling.

3.3 The solar cells shall be individually tested with the X-25L simulator lamp for electrical test on candidate solar cells. Select cells for Modules A and B, record and serialize.

3.4 The solar cells will be assembled into a 4-cell module. Figures 1 and 2 show front and back of the 4-cell test module. Figure 3 shows the module in an exploded view. Figure 3 is the proposed circuit design for connecting the 4 solar cells into a 4-cell series interconnected string.

3.5 The solar cells and substrates are mounted to the cell mounting frames in the solar array fabrication area.

- Serialize mounting frame useage for Modules B and C.
- Mechanically mount the thermocouples to the module frames, route the couple wires with stress relief, epoxy to their termination points.
- Make verification checks on each couple.
- Photographs - photos of test coupons and photos of test coupons in mounting frames.

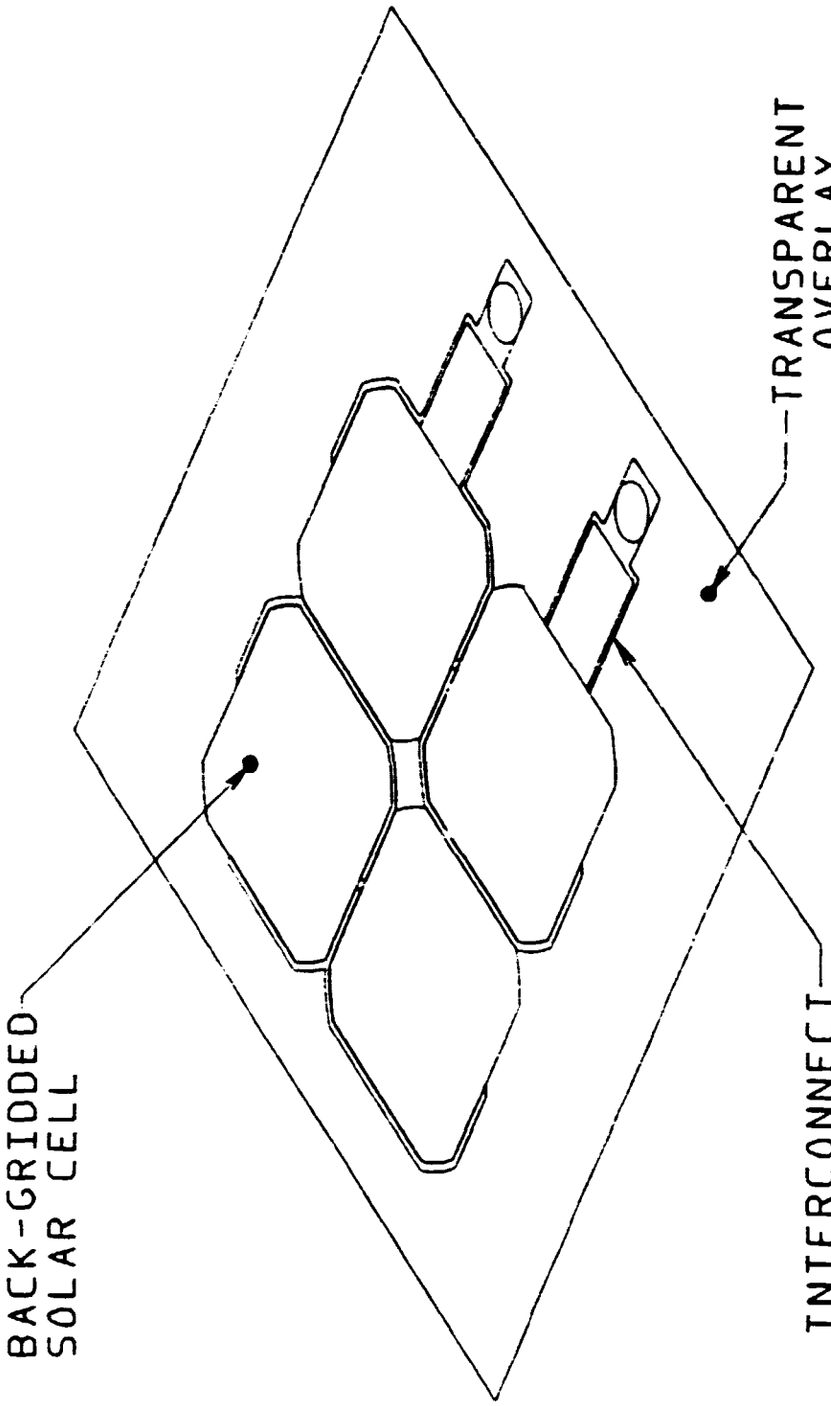

Figure 1 Transparent Module (Front View)

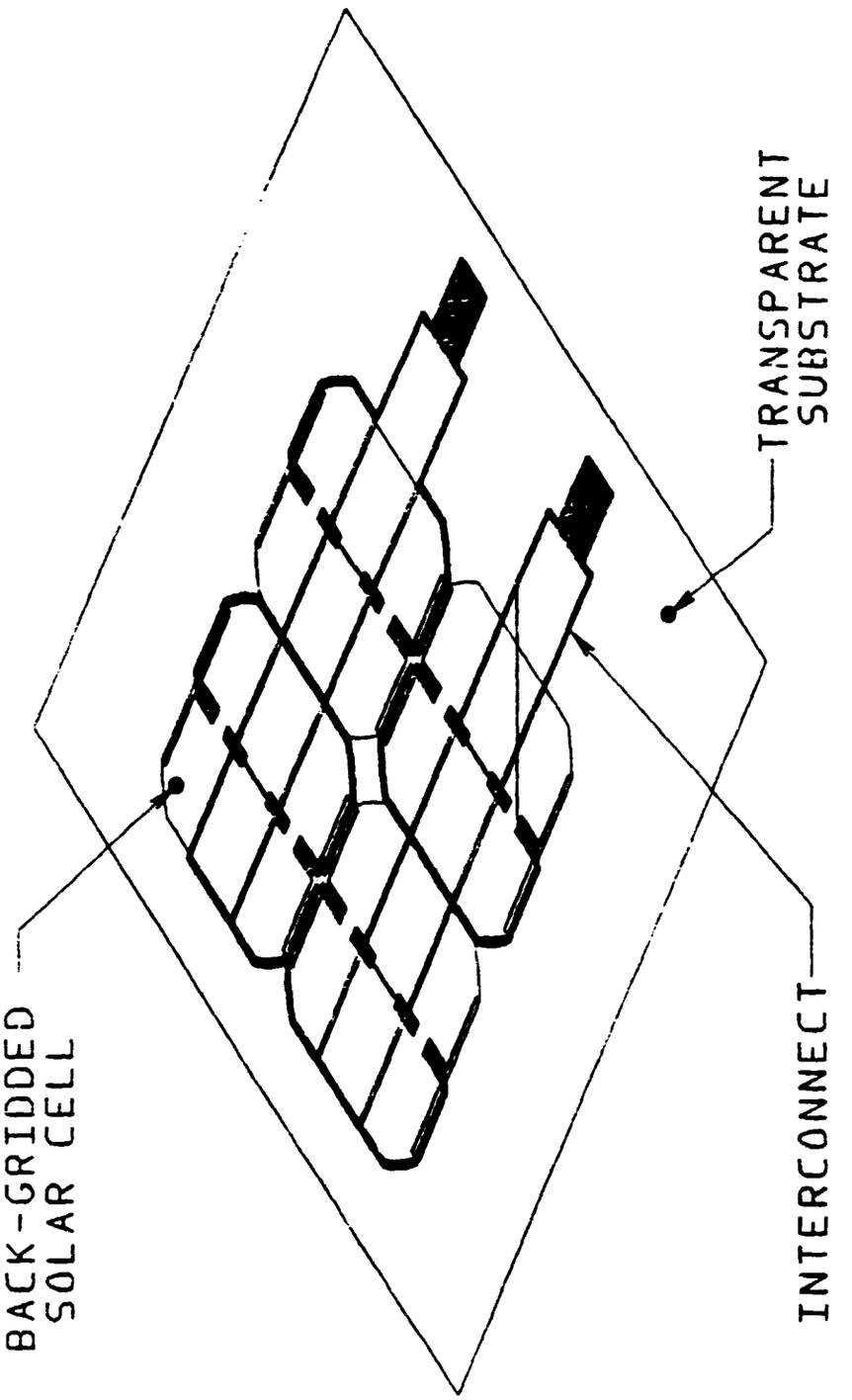

Figure 2 Transparent Module (Back View)

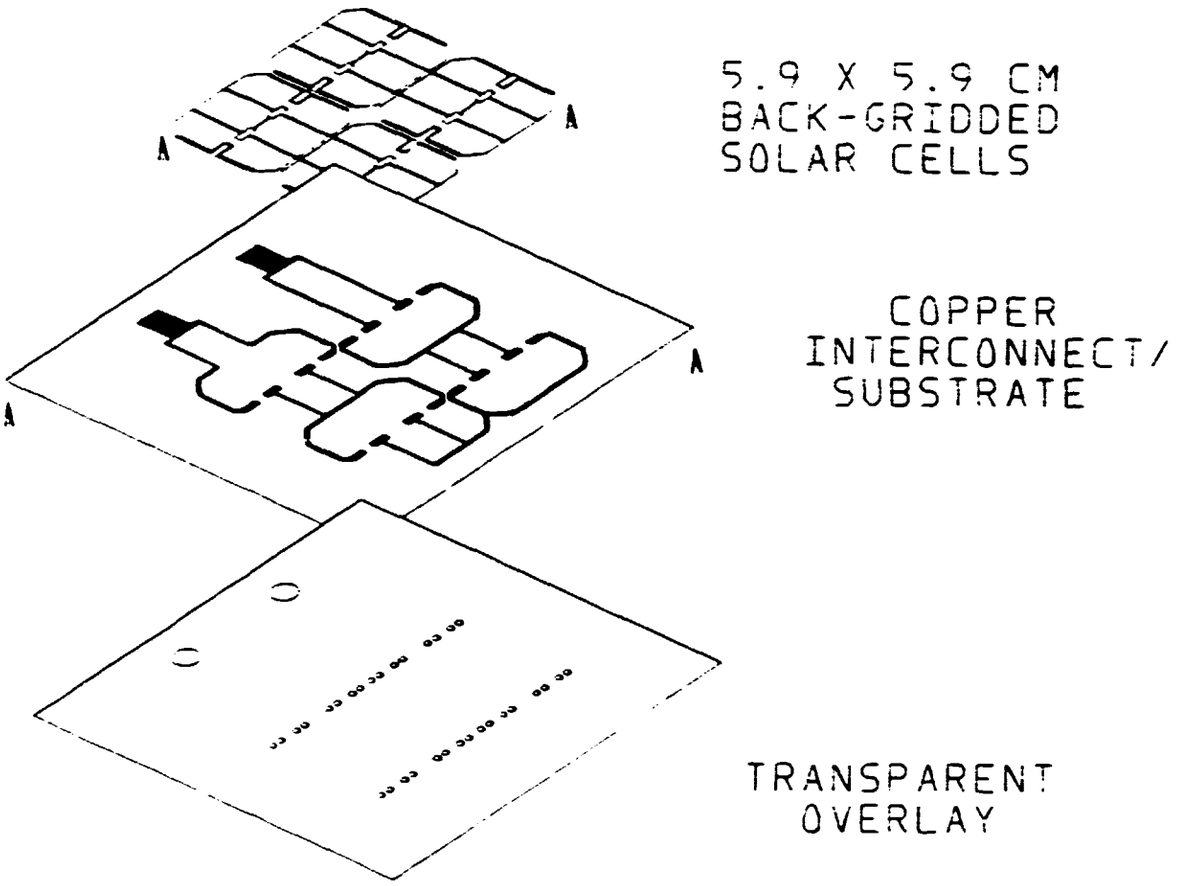

Figure 3 Transparent Module (Exploded View)

3.6 OPTICAL PROPERTIES MEASUREMENT

Measure reflectance ρ, transmittance τ, and absorptance α, as required.
Re-integrate for Xenon spectrum as required.

4.0 CHAMBER CALIBRATION

- Install one radiometer in chamber in test coupon location
- Pump down chamber to $\rho < 1 \times 10^{-4}$ torr
- Fill shrouds with LN_2
- Energize radiometer heater to levels .0677 W/m^2, 1353 W/m^2 and 2706 W/m^2. Allow to stabilize, record all thermocouples data. Repeat until all levels have been tested.
- Calculate background sink temperature and radiation interchange.
- Return chamber to ambient.
- Figure 4 shows a cross sectional plan of the radiometer.

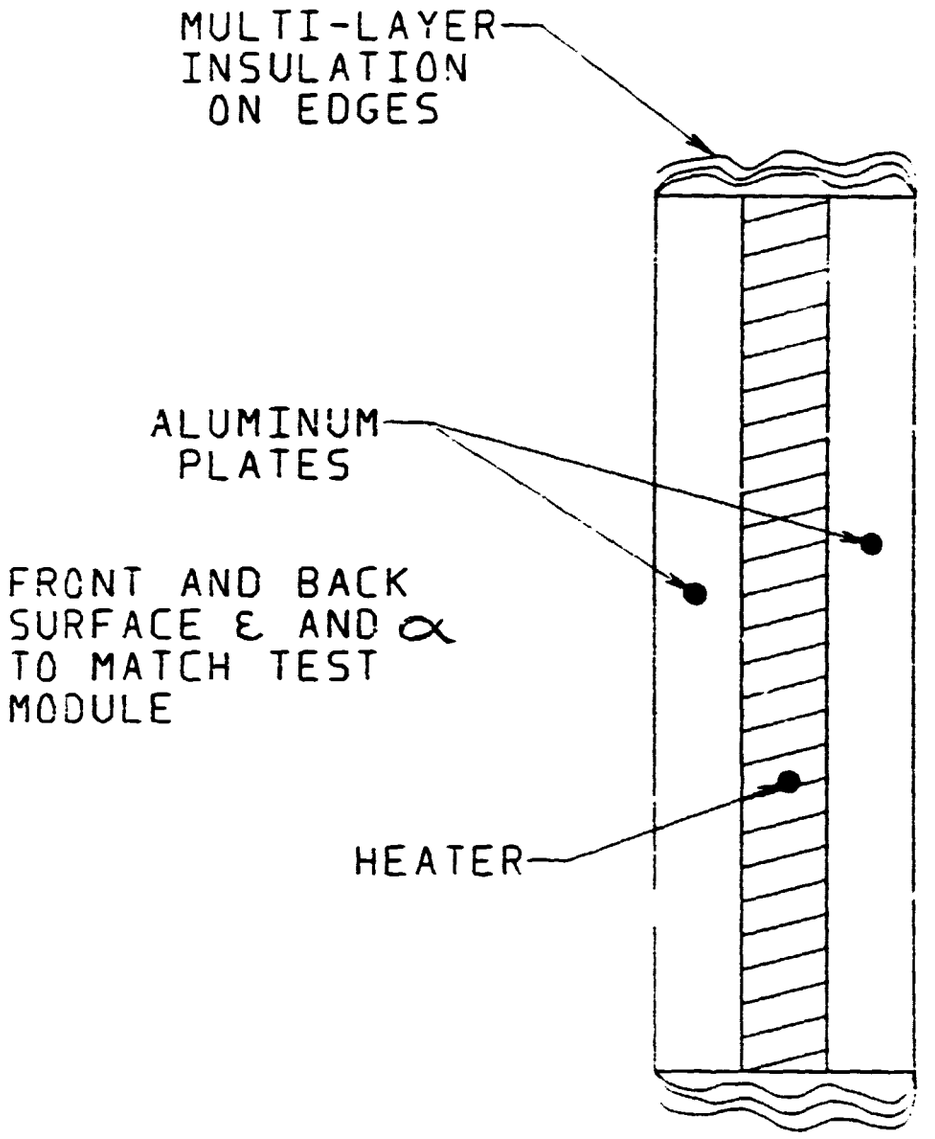

Figure 4 Radiometer Design

5.0 INSTALLATION OF TEST MODULE

- Table 1 is a list of the equipment to be used to support this test program. A schematic of test set-up in the space chamber is shown in Figure 5.

- The test module is vertically mounted inside space chamber no. 14 and completely surrounding the test sample is a Liquid-Nitrogen LN_2 shroud maintained at -300°F.

- The chamber shroud is painted black except for the 8.0 inch dia. clear aperture quartz window, that is 56.0 inches in front of the test module.

- The test module is illuminated with the X-25 Solar Simulator that is 92.0 inches in front of the test module.

TABLE 1
INSTRUMENTATION LIST

•	Fluke-Data Logger Model	Temperature Acquisition
•	Spectrolab-Electronic Load, Model	Test Sample Electrical Characteristics
•	Fluke-Digital Multimeter Model	V_{oc} and I_{sc}
•	Hewlett-Packard Moseley Plotter Model 1	X-Y Plotter for I-V Curves
•	Differential Radiometer Model TBD	Solar Irradiance
•	Beckman-Spectroradiometer Model	Solar Spectral Energy Distribution

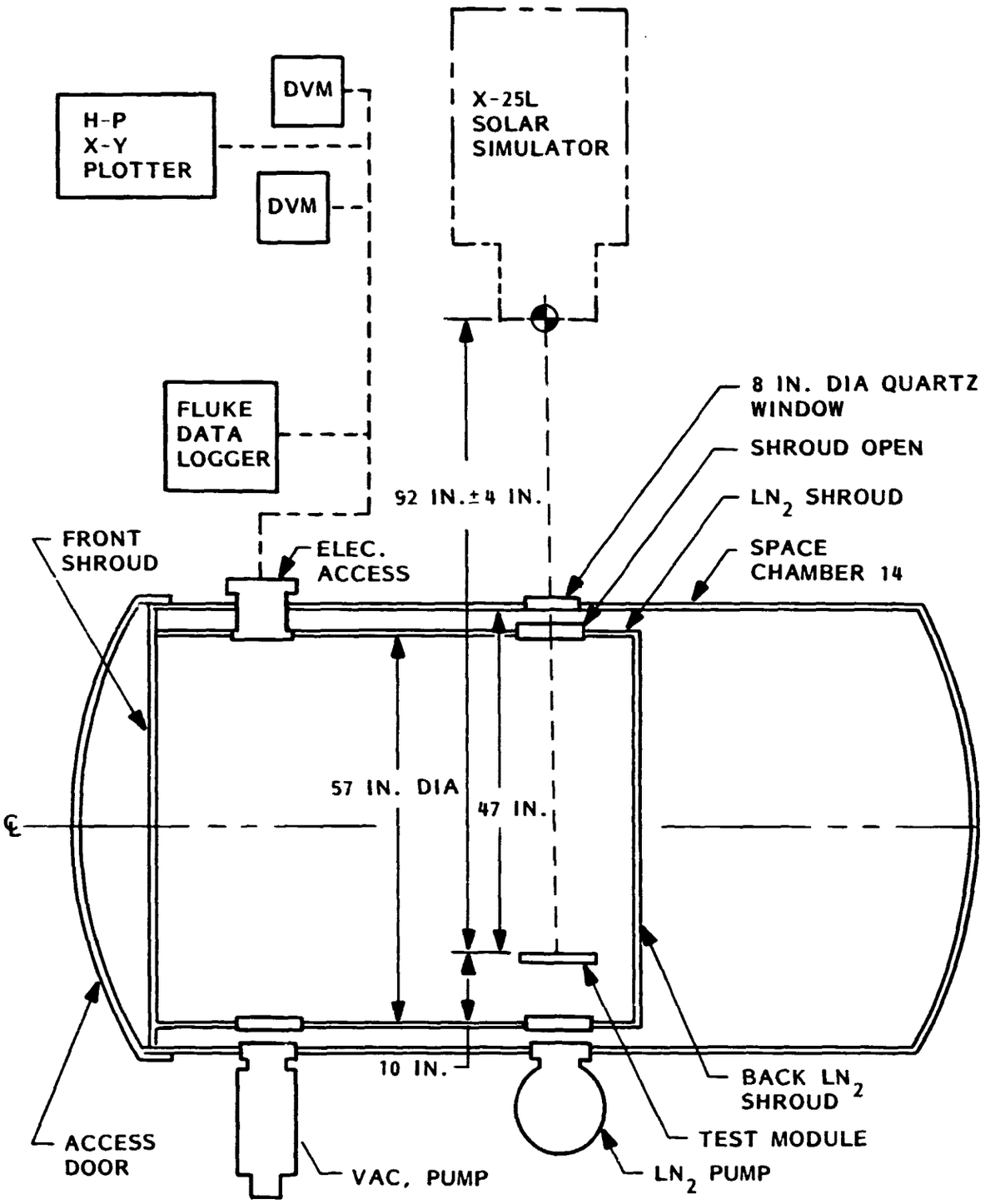

Figure 5 Schematic - Test Setup Space Chamber

6.0 SAMPLE TEST SUMMARY

a. Install Test Module A in chamber
b. Pump down chamber to $\rho < 1 \times 10^{-4}$ torr
c. Fill shrouds with LN_2
d. Set solar simulator intensity
e. Establish thermal equilibrium
f. Repeat as required (items a through e)
g. Electrical testing as required
h. Return to ambient

6.1 Energy reaching the specimen shall be determined by radiometric measurements.

- This knowledge shall be used in the thermal model for performance prediction.
- The actual samples will be instrumented to insure obtaining the actual solar cell temperature.
- The samples shall be calibrated such that Voc of the specimens can be used as an additional measurement of temperature.

6.2 THERMAL VACUUM TEST

1. Set up X-25 Solar Simulator and instrumentation in conjunction with space chamber No. 14 as indicated in Figure 5. The distance from the solar simulator to the test plane is 92.0 inches.

2. Mount Test Module A in the test plane and connect all thermocouples indicated in Figure TBD, test module thermocouple location to the data logger as indicated in Figure 6. Verify all electrical and thermocouples are indicating at the data logger.

TEST MODULE	THERMOCOUPLE NO.			
A	1	2	3	4
B	5	6	7	8
C	9	10	11	12

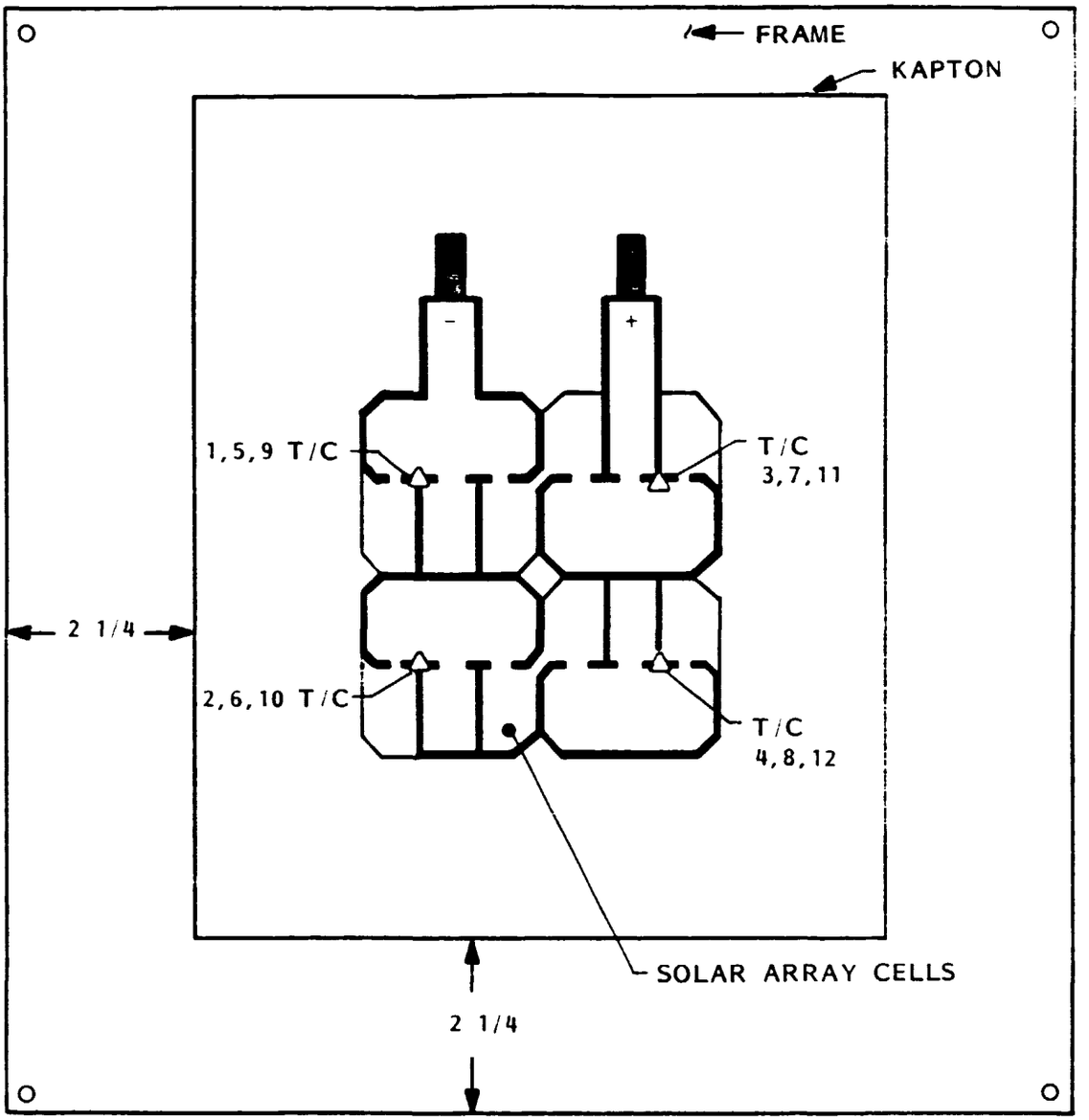

THERMOCOUPLES ON BACK OF KAPTON

Figure 6 Thermocouple Instrumentation - Back View

3. Pump the space chamber down to $\rho < 1 \times 10^{-4}$ torr. Before committing LN_2 to the shrouds, start the solar simulator and set the solar simulator intensity as indicated by the differential radiometer.

4. Start data logger recording at a sample rate of once per hour.

5. Commit LN_2 to shrouds and maintain chamber pressure at $\rho < 1 \times 10^{-4}$ torr.

6. Set data logger recording at a sample rate of once per minute and increase irradiance to 1353 W/m^2 (one sun). Verify all thermocouples on the test module are at a steady state condition for 15 minutes.

7. Record all data on data logger tape and attach to I-V curve.

8. Record the I-V electrical characteristics of the test module cells on the X-Y plotter. Indicate on curve the data, V_{oc}, I_{sc}, irradiance, scale, module letter, record in log book.

9. Determine the maximum power of the cells and set the electronic load at maximum power.

10. Determine that all temperature of the test module are at a steady state condition. (Note: Approximately 15 minutes). Record temperature readings and I-V characteristics.

11. Indicate on data logger tape the maximum power voltage and current, module letter, attach data logger tape of I-V curve and record in log book.

12. This completes this test cycle. Set solar irradiance at 700 W/m^2 and bring space chamber back to ambient conditions.

13. Repeat items 3 through 12 for 11 cycles.

14. Repeat Item 12.

15. Close beam douser and open door.

16. Repeat Items 1 through 15 for Test Modules B and C.

The test conditions are summarized below:

Test Facility	LMSC Solar Thermal Test Lab, Bldg. 104
Solar Source	SPL X-25 L Xenon Arc Solar Simulator with Filter System
Intensity Uniformity	± 2%
Intensity Stability	± 1%
Useable Beam Diameter	13"
Intensity Calibration	Radiometers
Vacuum Chamber	LMSC, Chamber No. 14
Wall Temperature	-300°F to -312°F
Thermocouple Channels	32
Test Date	February 13 through February 20, 1984

APPENDIX C

PRE-TEST THERMAL ANALYSIS

INTERDEPARTMENTAL COMMUNICATION

TXA-4007

TO	George Pack	DEPT./ ORGN.	62-16	BLDG ZONE	151	PLANT/ FAC.	1	DATE	7 February 1984
FROM	Kevin Freund	DEPT./ ORGN.	62-19	BLDG./ ZONE	104	PLANT FAC	1	EXT.	31361

SUBJECT THERMAL TEMPERATURE PREDICTION AND EVALUATION OF TEST CONFIGURATION OF TRANSPARENT SOLAR ARRAY

Ref:
(1) LMSC-D843553, Proposal for Demonstration of Transparent Solar Array Design 13 May 1983
(2) Project Description and Properties Figures, G. Pack, 10 January 1984
(3) Radiation Heat Transfer, E. M. Sparrow and R. D. Cess, 1966

SUMMARY

Predicted the solar cell surface temperature as a function of expected thermal-optical properties of the test sample for a range of incident radiation.

Evaluated chamber geometry and provided installation requirements to minimize sensitivity to test parameters. Provided thermo support for the use of a black plate radiometer to quantitatively evaluate cell transmittance and incident radiation. Required chamber calibration be conducted as referenced in LMSC-D843553 (Ref. 1).

OBJECTIVE

Perform hand calculations to determine solar cell surface temperature when subjected to space environment simulation. Surface temperatures plotted as a function of the expected ranges of cell absorption and transmittance, for incident radiation between one-half and two solar constants.

Determine sensitivity to test parameters such as location of sample in chamber and cold wall temperature. Evaluate the use of a simple black-plate radiometer to quantitatively determine cell transmittance. Provide thermo support for selection of size and placement.

Determine if a chamber calibration test should be conducted.

ANALYSIS

Hand calculations were performed to predict the solar cell surface temperature as a function of expected thermal-optical properties of the sample. The following three solar cell modules will be tested in a liquid nitrogen cold wall vacuum chamber.

Sample 1. Full Contact Back (Baseline Module)

Conventional silicon solar cell with a silver backing which will reflect the IR energy between $1 < \lambda < 4\mu$.

Sample 2. Conceptual Translucent Module

Gridded back solar cell bonded to a Kapton substrate which should transmit *85% IR energy $>1\mu$.

THERMAL TEMPERATURE PREDICTION AND EVALUATION OF TEST CONFIGURATION OF TRANSPARENT SOLAR ARRAY

Sample 3. GaAs/Silicon Translucent Module

Either a Ga-As translucent module or same as 2. But with Kapton substrate cut-away from cell back.

The thermal-optical properties of the cells used in this analysis (Ref. 2) are the following: the emissivity of cell front is .82 and cell back is .80. The cell absorption may vary between .5 and .75 and cell transmittance may vary between 0 and .4.

A simplified energy balance of the cell was performed assuming that the cell is isothermal at thermal equilibrium, and all energy absorbed is either converted to electrical power or is emitted to the chamber cold walls (see Analysis 1). The cell temperature is expressed as a function of cell transmittance and absorption by equations 1 and 2.

The reflectance of the solar cell was approximated by performing area integration under the monochromatic spectral reflectance curve and the normalized spectral response of the X-125 light spectrum (see Analysis 2). Assuming the calculated reflectance of .29 and a cold wall temperature of -300°F and substituting into equation 1 and 2 yields the baseline curves on Figures 1 and 2.

The radiation view factor sensitivity between the test panel and quartz window was evaluated as a function of placement depth of sample in chamber (Analysis 3). This analysis utilized the radiation view factor between parallel concentric discs of Ref. 3. The view factor sensitivity is illustrated as a function of placement depth of sample in chamber (Analysis 3).

The radiometer sensitivity to size and placement was calculated utilizing the radiation view factor equation for parallel concentric discs same as Analysis 3. The radiation view factor was calculated for radiometers between 1-3 cm in diameter and for locations less than 1 cm from test sample (see Analysis 4).

RESULTS AND CONCLUSIONS

The predicted solar cell surface temperatures are plotted as a function of the absorption coefficient ($\alpha - \eta$) and cell transmittance (τ) for incident radiation between one-half and two solar constants for cold wall temperature of -300°F (see Figs. 1 and 2). Figure 1 also illustrates the effect of cold wall temperature on cell surface temperature prediction. Figure 2 illustrates the effect of a $\pm 20\%$ error in calculated cell reflectance as calculated in Analysis 2.

The test configuration and chamber geometry is illustrated in Figure 3. To ensure predictable results, the following installation and mounting requirements are recommended.

- The test sample should be placed as deep as possible in chamber (see Fig. 3) about 47" from quartz window, to minimize port view factor as illustrated in Analysis 3.
- Test sample should be mounted on port centerline and perpendicular to the source to ensure equal distribution of reflected intensity.
- The X-125 light source should be placed between 90" - 96" from the sample and chamber calibration is required to ensure a 13" minimum diameter is projected through the 8" diameter quartz window.

THERMAL TEMPERATURE PREDICTION AND EVALUATION OF TEST CONFIGURATION OF TRANSPARENT SOLAR ARRAY

The simple black plate radiometer may be used to evaluate cell transmittance and the incident radiation intensity if the following provisions are observed:

- Radiometer is constructed of a material sensitive to the total IR spectrum and should be as thin as possible to minimize thermal lag.
- Radiometer size and placement should be selected to minimize radiometer to cell view factor sensitivity as illustrated in Analysis 4. The radiometer size should not exceed 2 cm diameter and should be placed within 1/2 cm from cell back.
- Radiometer should be placed as close as possible to the cell and should remain constant for each test being conducted.
- The radiometer mounting fixture should be constructed of low-conductive material to minimize conduction losses.
- When radiometer is selected, Thermo should review selection to ensure conformance with design requirements.

Chamber calibration must be conducted as described in LMSC-D843553 (Ref. 1). This calibration procedure should also include spectrum analysis of the X-125 light source for wavelengths $.1 < \lambda < 4\,\mu$.

APPROVED BY:

/original signed/

G. D. Bizzell, Manager
Thermodynamics

PREPARED BY:

/original signed/

K. D. Freund
Thermodynamics

cc;
G. D. Bizzell 62-19/104
J. Lilly 62-16/151

ANALYSIS 1 – CELL TEMPERATURE

Hand calculations to evaluate solar cell temperature as a function of cell thermal-optical properties and incident radiation.

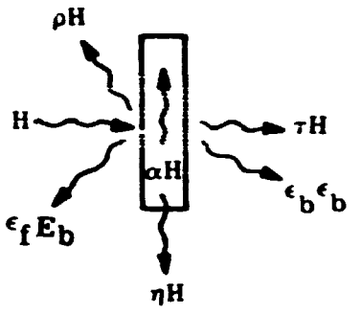

H	=	Incident Radiation
ρ	=	Reflectance
α	=	Absorption
τ	=	Transmittance
ϵ_f	=	Emissivity of Front
ϵ_b	=	Emissivity of Back
η	=	Electrical Efficiency
T_c	=	Temperature of Cell
T_∞	=	Cold Wall Temperature

ASSUMPTIONS:

1. Cell is Isothermal and at Steady State
2. Reflectance and Emittance Diffusely Distributed
3. No Conductive or Radiation Losses from Cell Edges
4. Neglect Radiation Exchange with Chamber Port
5.

Energy Balance $\Sigma E_{in} = \Sigma E_{out}$

$$H = (\epsilon_f + \epsilon_b)\,\sigma\left(T_c^4 - T_\infty^4\right) + H\,(\rho + \tau + \eta)$$

Solving For T_c

(1) $$T_c = \left[H(1-(\rho + \tau + \eta))/(\epsilon_f + \epsilon_b)\,\sigma + T_\infty^4\right]^{1/4}$$

If $\alpha + \rho + \tau = 1$ Then $\alpha = 1 - \rho - \tau$

(2) $$T_c = \left[H\,(\alpha - \eta)/(\epsilon_f + \epsilon_b)\,\sigma + T_\infty^4\right]^{1/4}$$

ANALYSIS 2 – CELL REFLECTANCE

Evaluation of average cell reflectance from cell reflectance data.

$$\frac{\int_0^\infty \rho(\lambda)\, G(\lambda)\, d\lambda}{\int_0^\infty G(\lambda)\, d\lambda}$$

ρ = Data Figure

G = Data Figure

Area integration of cell spectral reflectance and the normalized solar spectrum.

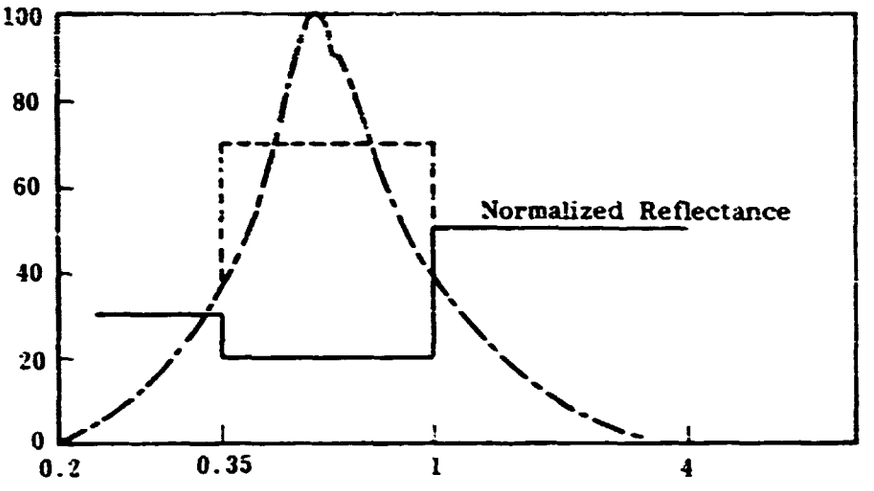

$$\int_0^{.35} \rho(\lambda)\, G(\lambda)\, d\lambda + \int_{.35}^{1.1} \rho(\lambda)\, G(\lambda)\, d\lambda$$

$$+ \int_{1.1}^{\infty} \rho(\lambda)\, G(\lambda)\, d\lambda \;/ \int_0^{\infty} G(\lambda)\, d\lambda$$

$$\rho = \left[30\ (\tfrac{1}{2} \times 15)\ (40) + 20\ (.75)\ (70) + 50\ (\tfrac{1}{2})\ (3)\ (40)\right] / 100$$

ρ = 0.29 (average reflectance)

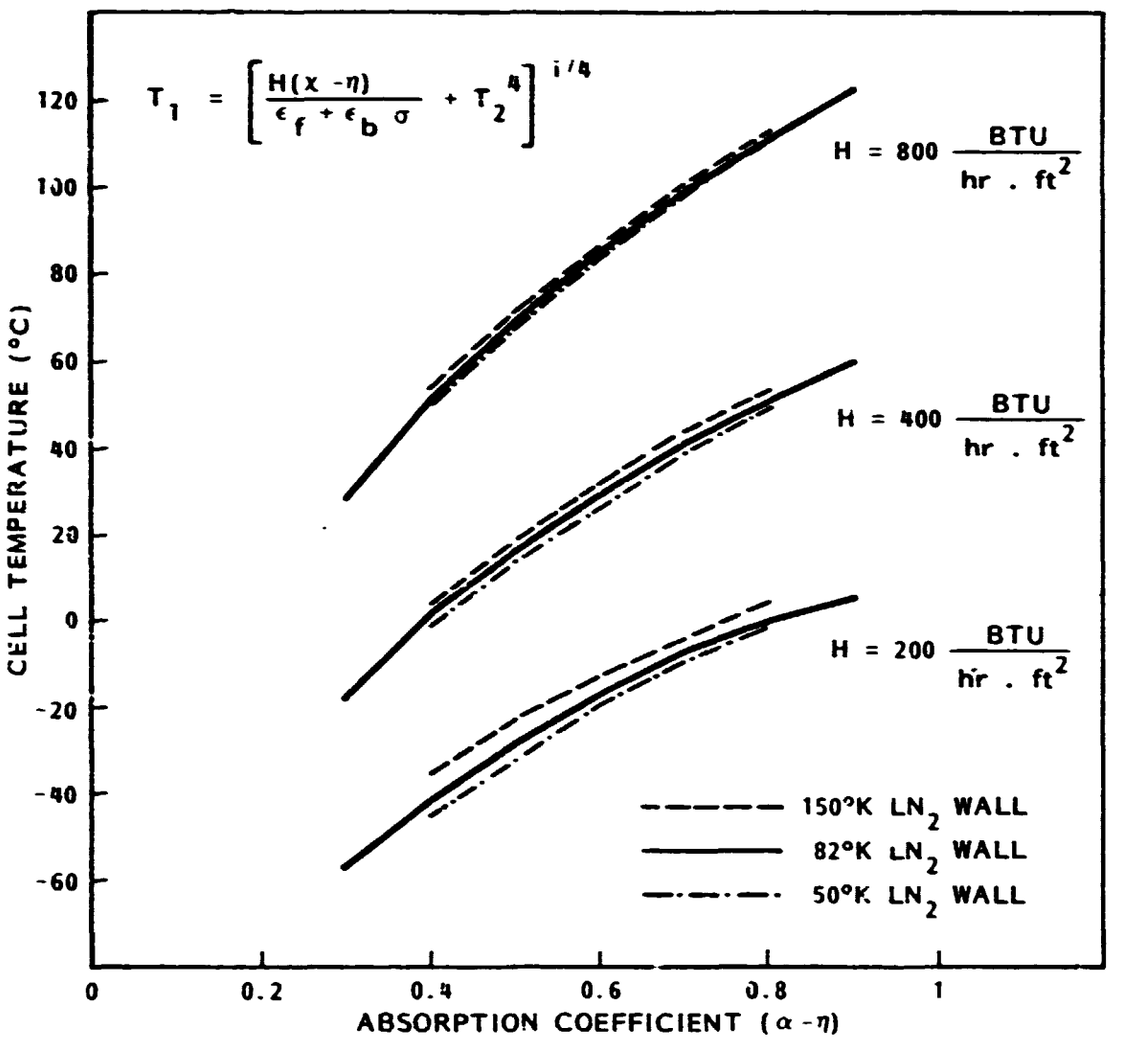

Figure 1 Solar Cell Temperature versus Cell Absorption Coefficient

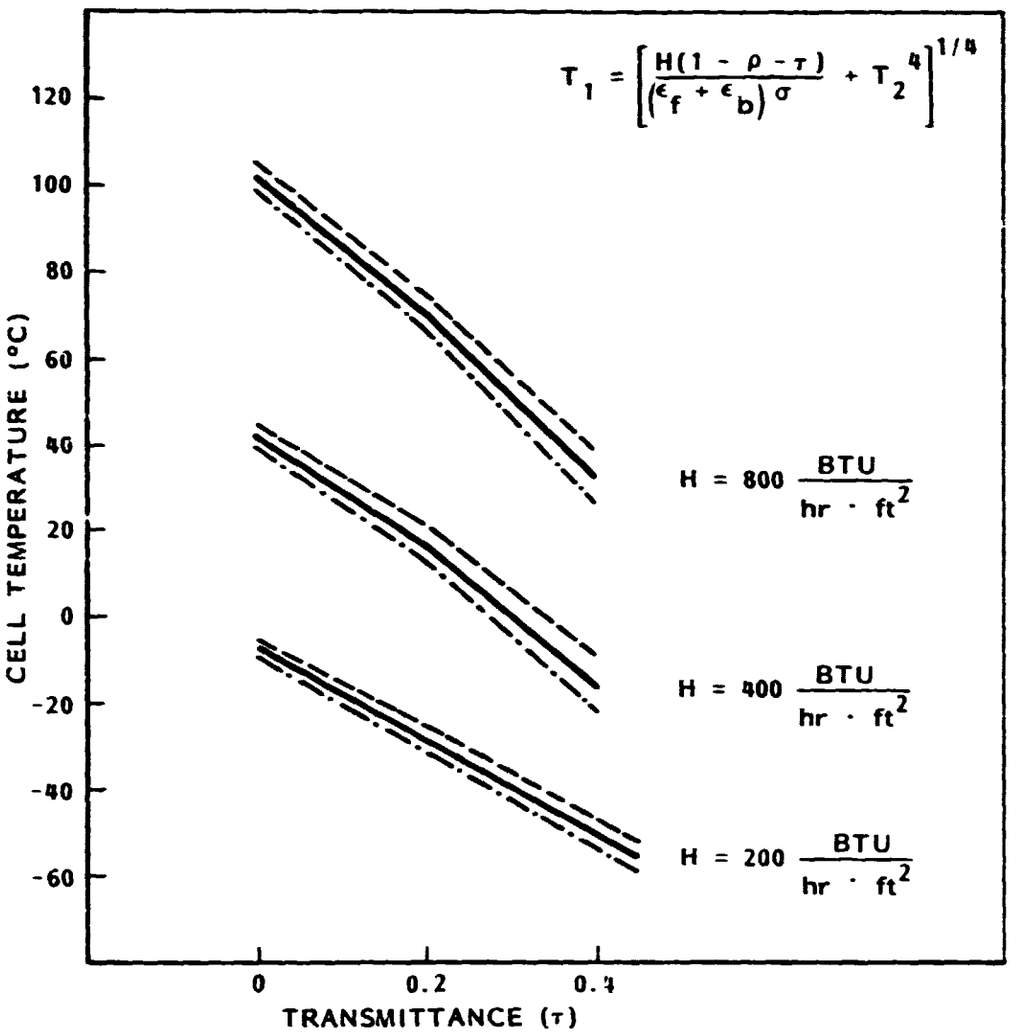

Figure 2 Solar Cell Temperature versus Cell Transmittance

ANALYSIS 3 – CELL CHAMBER PLACEMENT SENSITIVITY

Determine view factor sensitivity to placement of test sample in chamber.

Given:

13" diameter test panel to 8" diameter quartz window for a 48" max chamber depth

Radiation view factor for parallel concentric discs. (Ref. 3)

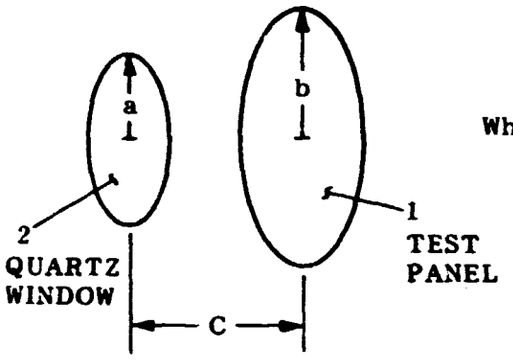

$$F_{1-2} = 1/2\left(Z - \sqrt{Z^2 - 4X^2Y^2}\right)$$

Where

$X = a/c$ and $Y = c/b$

$Z = 1 + (1+X^2)\,Y^2$

$a = 8"/2 = 4"$

$b = 13"/2 = 6.5"$

Test Panel to Window View Factor
vs
Distance From Panel to Window

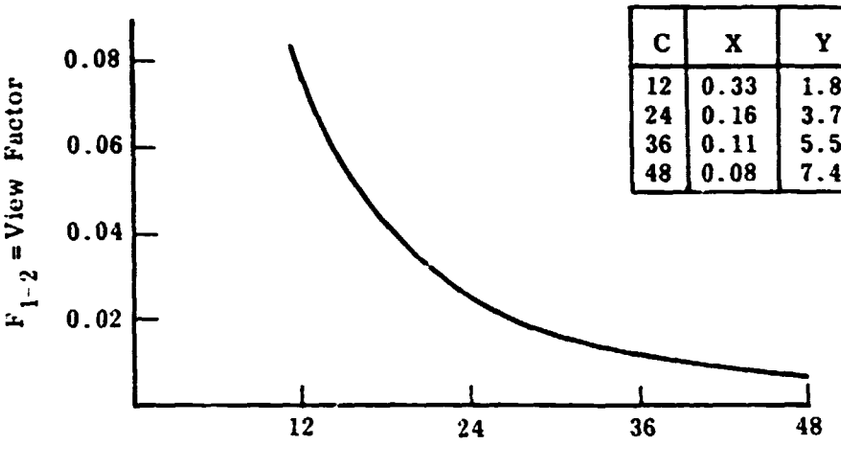

C	X	Y	Z	F_{1-2}
12	0.33	1.8	4.8	0.08
24	0.16	3.7	15.0	0.025
36	0.11	5.5	32.0	0.012
48	0.08	7.4	55.9	0.007

ANALYSIS 4 – RADIOMETER SIZE AND PLACEMENT SENSITIVITY

Determine view factor sensitivity of a simple black plate radiometer size and placement. Utilizing radiation view factor between parallel concentric discs (Ref. 3).

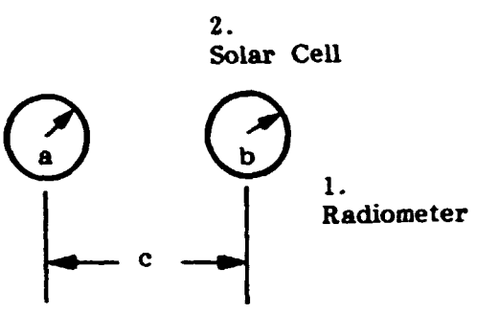

$$F_{1-2} = 1/2 \left(Z - \sqrt{Z^2 - 4X^2Y^2} \right)$$

Where

$X = a/c$ and $Y = c/b$

$$Z = 1 + \left(1 + X^2\right) Y^2$$

a = Cell Radius = 1.45 cm

b = Radiometer Radius

c = Radiometer Distance

F_{1-2} = View Factor 1-2

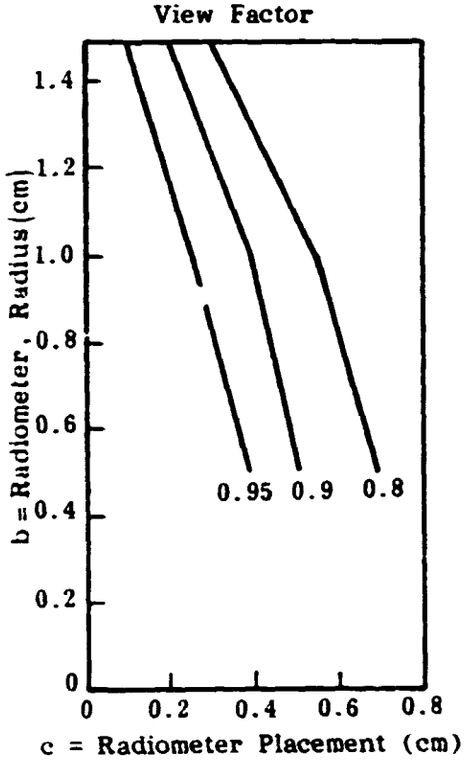

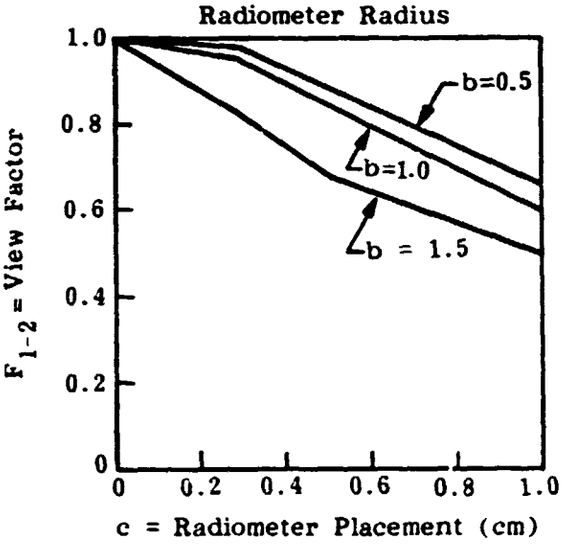

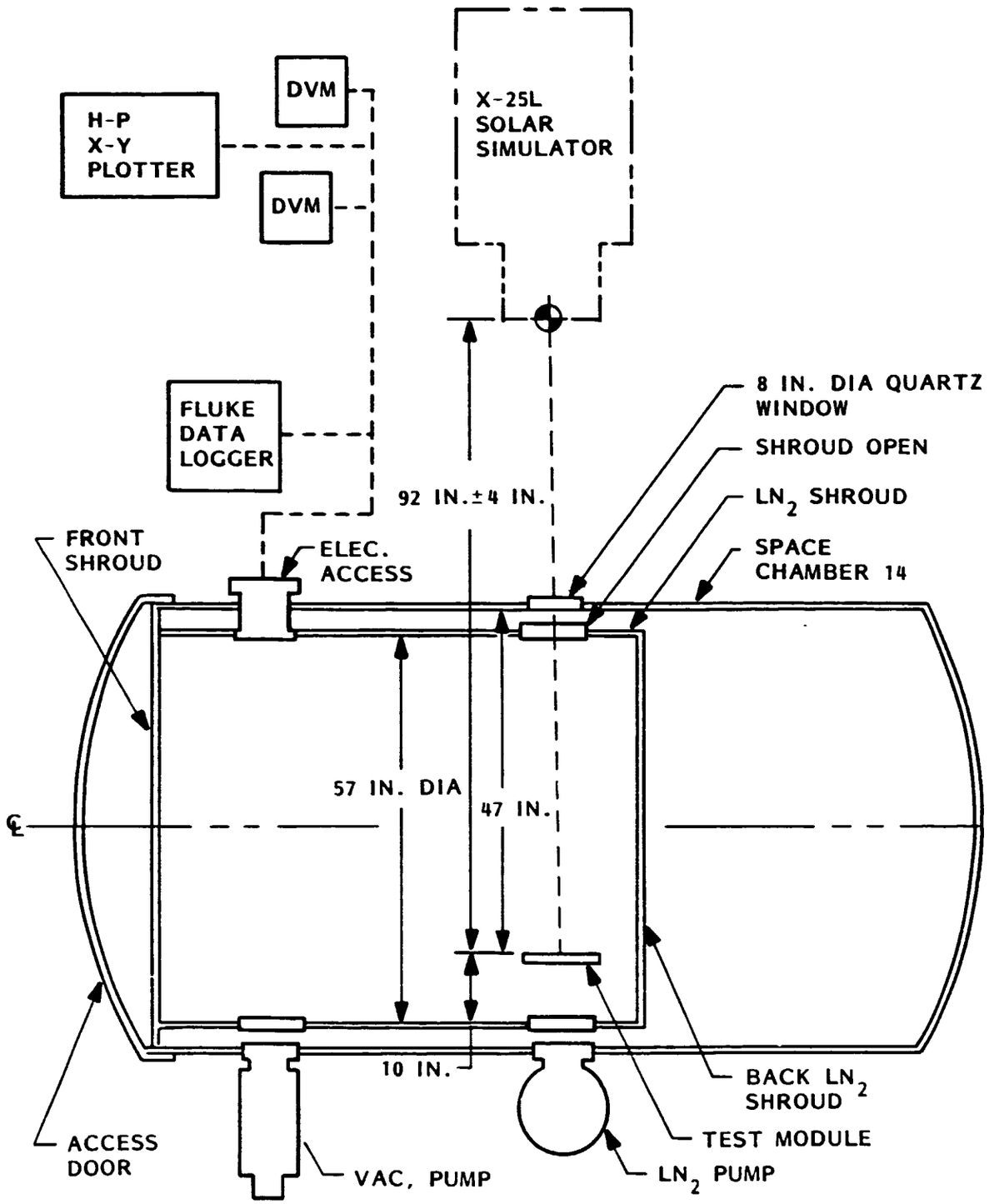

Figure 3 Schematic - Test Setup Space Chamber